

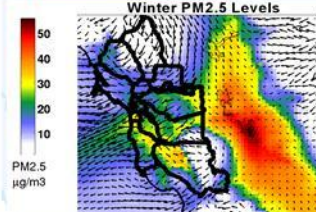
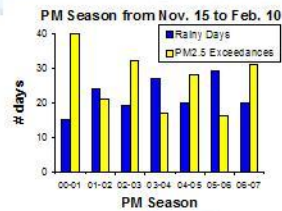
BAY AREA
AIR QUALITY
MANAGEMENT
DISTRICT

939 Ellis Street, San Francisco, CA 94109

Research and Modeling Section Publication No. 200906-002-TX

Toxics Modeling to Support the Community Air Risk Evaluation (CARE) Program

June, 2009



Prepared by:

Saffet Tanrikulu, Research and Modeling Manager
Phil Martien, Senior Advanced Projects Advisor
Cuong Tran, Senior Atmospheric Modeler

Significant contributors:

Yiqin Jia, BAAQMD
David Fairley, BAAQMD
Amir Fanai, BAAQMD
Jeff Matsuoka, BAAQMD
James Cordova, BAAQMD
Chris Emery, ENVIRON International Corporation
Stephen B. Reid, Sonoma Technology, Inc.

Reviewed and approved by:

Henry Hilken, Director of Planning, Rules and Research Division

Executive Summary

This report presents regional toxics modeling conducted by the Bay Area Air Quality Management District (BAAQMD) in support of the Community Air Risk Evaluation (CARE) program. The BAAQMD started the CARE program in 2004 to estimate and reduce health risks associated with exposure to outdoor toxic air contaminants (TAC) within the Bay Area. The CARE program's toxics modeling was initiated by the California Air Resources Board (ARB) over West Oakland, using the CALPUFF model, about three years later. Subsequently, ENVIRON International Corporation simulated regional toxics concentrations over core areas of the Bay Area. District staff built on ENVIRON's work by simulating toxics concentrations over the entire Bay Area and calculating the associated cancer risk for Bay Area residents.

For this effort, meteorology from 2000 and emissions inventory from 2005 (Appendix A) were used. The selected models were the Mesoscale Meteorological Model version 5 (MM5) for meteorological modeling (Appendix B) and the Comprehensive Air Quality Model with Extensions (CAMx) for ozone and toxics modeling (Appendices C and D). These two models are highly sophisticated and preferred for most model applications in the nation. The emissions inventory used was the best available for the region.

Toxics species like formaldehyde, acetaldehyde, etc. can undergo chemical reactions in the atmosphere and form secondary pollutants in addition to their direct emissions into the atmosphere. Atmospheric oxidants play an important role in secondary toxics formation. These oxidants are essentially the products of ozone chemistry. Therefore, ozone chemistry was included in the toxics simulations.

To meet the CARE program's objectives, two sets of toxics simulations were performed: 1) with diesel particulate matter emissions (DPM) only and 2) with reactive toxics species emissions.

The simulations with DPM only included emissions from all diesel sources in the Bay Area. Two periods July 12-18 and December 12-18, 2000 were simulated and average diesel PM concentrations were calculated. The annual average concentration is assumed to be 96% of the average of these two periods. The 96% factor was determined by comparing July and December observed CO average concentrations to annual average CO concentrations (See Appendix E for details).

Figure ES1 shows the distribution of simulated annual average PM concentrations from DPM. The highest annual average concentration was located over West Oakland (10-12 $\mu\text{g}/\text{m}^3$), extending toward Emeryville and along both sides of the eastern span of the Bay Bridge. The second highest (8-10 $\mu\text{g}/\text{m}^3$) were over West Oakland, south-east of downtown Oakland, Alameda, and the Transbay District/Rincon Hill areas in San Francisco. Several grid cells with concentrations ranging from 4 to 8 $\mu\text{g}/\text{m}^3$ exist just outside of these regions.

Concentrations from 2 to 4 $\mu\text{g}/\text{m}^3$ cover an area from the Berkeley Marina in the north to San Leandro in the south and from downtown San Francisco in the west to Piedmont in the east. Areas just north and east of downtown San Jose also have an annual average concentration of 2-4 $\mu\text{g}/\text{m}^3$. Concentrations from 1 to 2 $\mu\text{g}/\text{m}^3$ cover an area from Richmond in the north to San Jose in the south and from San Francisco in the west to Piedmont in the east, mostly around freeways. Similar concentrations were estimated along portions of SR-4, I580 and I-680, as shown in the figure.

The full chemistry toxics simulation included all known major carcinogenic toxics emissions in the Bay Area. The initial and boundary conditions were set to a small, near zero numbers to avoid potential numerical problems. The full chemistry runs covered seven-day periods for summer (July 12-18) and for winter (December 12-18). The selected periods were average summer and winter days from the meteorological perspective; however, observations showed December 2000 was, in general, an above-average PM month. Additionally, PM concentrations in mid-December are generally higher than other winter periods. Therefore, the simulated toxics concentrations were expected to represent high-end winter concentrations.

Next, a combined cancer risk from five toxics species (diesel PM, 1,3-butadiene, benzene, formaldehyde, and acetaldehyde) was calculated over the entire modeling domain. Other modeled carcinogenic toxics species were not included in this calculation either because their concentrations were too low or their unit risk factors were too small. The unit risk factors (OEHHA, 2002) used for the above species were 300, 170, 29, 6, and 2.7 cancer per million per $\mu\text{g}/\text{m}^3$, respectively.

Cancer risk for each species above was calculated by multiplying their respective annual average concentrations with their unit risk factors and then summing the resulting values. The results were expressed as the number of expected cancer incidences per million people and plotted in Figure ES2. West Oakland had the highest number of expected cancer incidences of around 3,000 per million. Downtown San Francisco was second with a number around 2,500 per million. Expected incidences in the range of 2,250 to 2,500 per million were located over an area extending from Emeryville in the north to Alameda in the south and from West Oakland in the west to the I-580 corridor in the east. Similar numbers were also found in downtown Oakland. Expected incidences ranging from 500 to 1000 per million covered an area from Richmond in the north to San Jose in the south and from San Francisco in the west to the East Bay Hills in the east, with Oakland connected to San Jose along the I-880 corridor. Much of the Bay and its surrounding areas, including Santa Rosa, Travis Air Force Base, and portions of the SR-4, SR-24, I-80, I-580 and I-680 corridors had expected incidences ranging from 250 to 500 per million.

The expected cancer incidences were then adjusted from per million to actual Bay Area populations. This was done by multiplying the expected incident number of each grid cell by the actual population of that cell and dividing the result by one million. The adjusted cancer risks are shown in Figure ES3.

The population-adjusted expected incidences spatial distribution was similar to the number of expected incidences per million people. However, some shift in the distribution was evident. The highest number of population-adjusted incidences was around 40, occurring over a grid cell in downtown San Francisco. The second highest number of around 25 was also in downtown San Francisco, extending toward Civic Center. Population-adjusted expected incidences around 15 were found in east Oakland and west and south of the San Francisco Civic Center. Expected incidences around 10 were found in much of Oakland and a small portion of San Francisco. Incidences around 5 were found in an area from Richmond and San Francisco in the north to San Jose in the south, mostly following the major freeways.

The population-adjusted cancer incident numbers were further modified based on the sensitive population defined as people over 64 and under 18. The resulting distribution of expected incident numbers is displayed in Figure ES4. The highest expected incident number was around 10, located over downtown Oakland and San Francisco. The number around 5 covers much of downtown Oakland, downtown San Francisco, and a small part of east San Jose.

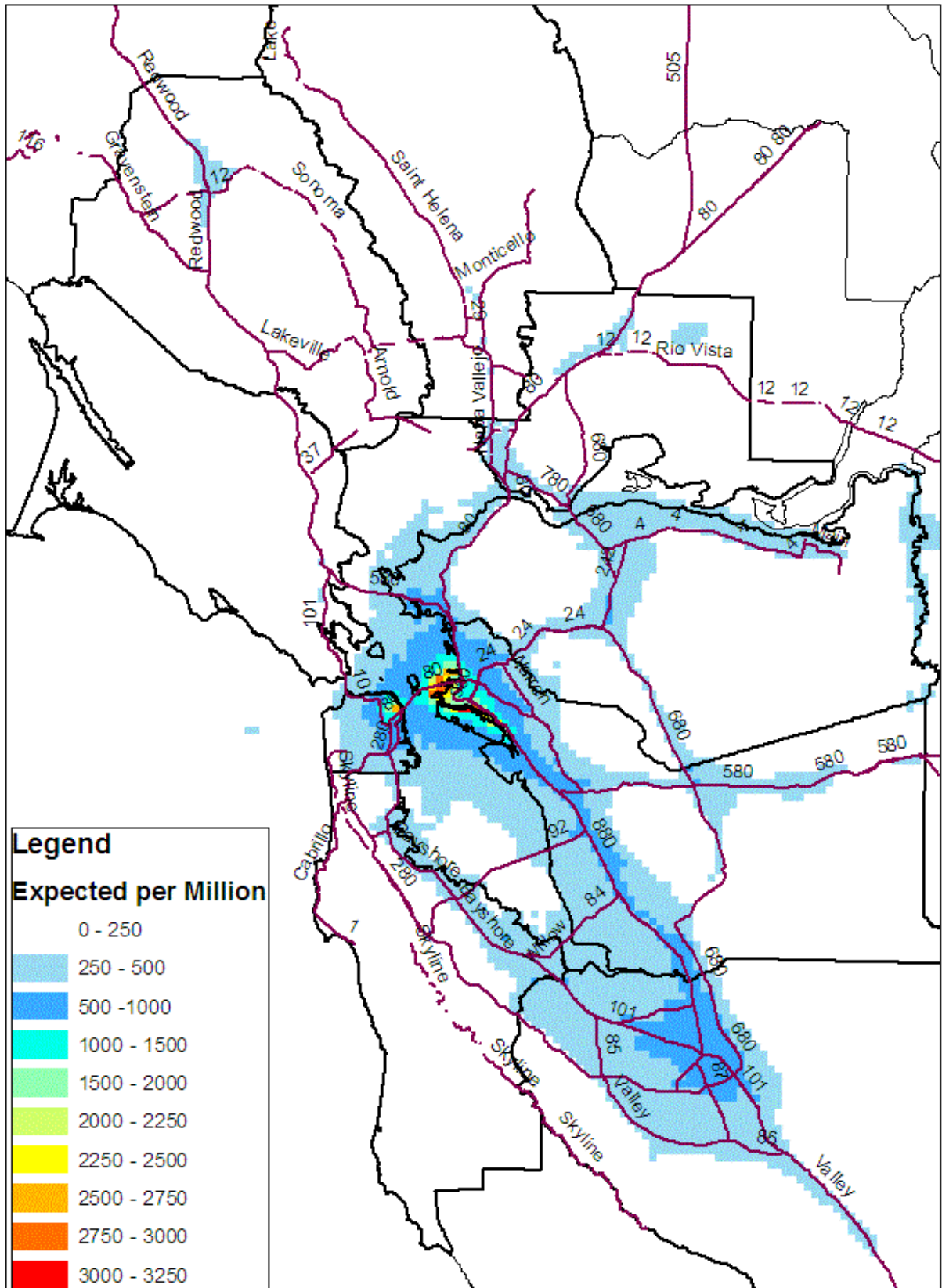


Figure ES2: Expected number of cancer incidents per million.

Toxics Modeling to Support the Community Air Risk Evaluation (CARE) Program

1. Introduction

This report presents technical details of toxics modeling conducted by staff of the Bay Area Air Quality Management District (BAAQMD) in support of the Community Air Risk Evaluation (CARE) program. The BAAQMD started the CARE program in 2004 to estimate and reduce health risks associated with exposure to outdoor toxic air contaminants (TAC) within the Bay Area. The CARE program's toxics modeling was initiated by the California Air Resources Board (ARB) over West Oakland, using the CALPUFF model, about three years later. Under this effort, the annual average ambient concentrations of selected toxics species were simulated using year-2000 emissions and cancer risk was evaluated for West Oakland residents. Subsequently, the BAAQMD established a contract with ENVIRON International Corporation (ENVIRON; ENVIRON, 2008) to conduct regional toxics modeling over the Bay Area, using meteorological inputs generated by ARB and emissions inputs generated by Sonoma Technology, Inc. (STI; STI, 2006).

Under this effort, ENVIRON simulated ambient concentrations of selected toxics species, using the Comprehensive Air Quality Model with Extensions (CAMx). ENVIRON evaluated CAMx's performance, improved its toxics chemistry module for the Bay Area, and delivered the resulting model inputs and outputs and the source code to the District. The District's modeling and CARE staff extensively evaluated the delivered products and identified two major areas for improvements, both in the meteorological inputs: 1) the meteorological modeling domain was too small, not covering the entire Bay Area, especially Santa Clara County. As a result, the accompanying CAMx domain did not meet the CARE program's regional toxics modeling needs. 2) On certain days, the simulated wind speed was too strong, significantly impacting the performance of CAMx.

In order to overcome these shortcomings, District staff simulated meteorology over the entire Bay Area, using both the Mesoscale Meteorological Model version 5 (MM5) and the California Meteorological Model (CALMET), which was used by ARB. Comparison of wind fields obtained from these two models against observations showed that the performance of MM5 was superior to CALMET. Therefore, the MM5 was selected to prepare meteorological inputs to CAMx.

By the time the meteorological modeling was completed, STI updated the CARE emissions inventory from 2000 to 2005 (STI, 2008). This updated inventory was also selected for toxics simulations. The following sections of this report detail the emissions inventory preparation, meteorological modeling, toxics modeling and the analysis of resulting toxics concentrations and risk assessments. Spatial distributions of emissions of selected toxics species and their county totals are given in Appendix A. Meteorological model (MM5) evaluation against

observations is given in Appendix B. Air quality model (CAMx) model evaluation against observations is given in Appendix C. Technical details of how toxic air contaminants were simulated are presented in Appendix D.

2. Emissions Inventory Preparation

Emissions estimates of toxic pollutants and ozone precursors were prepared as inputs to CAMx. To ensure timely availability of the input files, the District obtained assistance from STI. STI's main involvement (STI, 2008) was to process the 2005 CARE emissions inventory for use in the U.S. EPA's Sparse Matrix Operator Kernel Emissions (SMOKE) computer program. SMOKE was then used by District staff to generate the CAMx inputs.

Emissions for TOG and the criteria pollutants NO_x, CO, SO₂, and PM₁₀ were added to the 2005 toxics emissions database in order to create a model-ready inventory. The addition of TOG and NO_x emissions, in particular, were needed because they participate in photochemistry affecting the organic toxics' concentrations. Emissions inputs from biogenic sources were prepared using a method developed by ARB.

The area and non-road mobile source data in the CARE inventory were given as annual average daily totals by county. First these emissions were reformatted for input to SMOKE. Then using SMOKE, they were distributed spatially, temporally, and chemically to 1-km grid cells, using surrogates provided by STI (STI, 2006). Since CAMx modeling was performed for July and December, two separate emissions inventories were prepared for these two months. SMOKE was further applied to adjust the annual average emissions for seasons.

To prepare the CAMx ready on-road mobile source emissions inventory, emissions from these sources were first gridded and temporally allocated using the California Department of Transportation's (CalTrans) Direct Travel Impact Model (DTIM). The rest of the processing and adjustments were made using SMOKE.

The CAMx-ready stationary point source emissions included emissions from all permitted sources as well as necessary meteorological information and stack parameters for CAMx to estimate plume rise for each source.

In this model application, anthropogenic emissions were only from the Bay Area sources, while biogenic emissions included the Bay Area and portions of the northern San Joaquin Valley and the Sacramento area to carry out chemical reactions beyond the District boundaries.

3. Modeling

3.1 Meteorological Modeling

Four nested domains were used for meteorological modeling. The outer domain covered the entire western U.S. with 36-km horizontal grid resolution to capture synoptic flow features and the impact of these features on local meteorology. The second domain covered California and portions of Nevada with 12-km horizontal resolution to capture mesoscale flow features and their impact on local meteorology. The third domain covered the Bay Area, northern San Joaquin Valley, and Sacramento area as well as portions of the Pacific Ocean with 4-km resolution to capture local air flow features. The innermost domain, which was used for CAMx simulations, covered just the Bay Area and had 1-km resolution with 152 grid cells in the east-west direction and 208 grid cells in the north-south direction. All four domains employed 50 vertical layers whose thicknesses expanded with height from the surface to the top of the modeling domain (about 16 km). In MM5, meteorological variables are estimated at the middle of the layers. The thickness of the first layer near the surface was about 22 m; thus meteorological variables near the surface were estimated 11 m above the ground level in this application. The physics options selected in MM5 were similar to those used by the National Oceanic and Atmospheric Administration (NOAA) for the Central California Ozone Study simulations. These options were well tested and proven to be the best options to characterize meteorology in the region. The simulated winds were nudged toward surface observations obtained from National Weather Service stations.

Simulation periods were July 12-18 and December 12-18, 2000. The resulting meteorological fields were compared against observations as well as the results obtained from CALMET. In general, MM5 replicated meteorology better than CALMET.

3.2 Toxics Modeling

The toxics modeling domain was centered in the innermost meteorological modeling domain with 140x196 horizontal grid cells and 1-km grid resolution. Following this approach, the meteorological fields from six grid cells along the edges of the meteorological modeling domain were not used in order to minimize the impact of boundary conditions with the 4-km modeling domain on toxics modeling. In aloft layers, some meteorological model layers were combined in preparing meteorological inputs to CAMx to reduce computational time. This is a common practice in air quality modeling as pollutant concentrations in aloft layers are relatively low and do not significantly impact concentrations at the surface. The resulting number of vertical layers in CAMx was 20, with layer thicknesses also expanded with height from the surface to the top of the modeling domain (about 16 km). The thickness of the first layer of CAMx was kept the same as MM5's (about 22 m), estimating pollutant concentrations at 11 m above the surface.

Some toxics species, like formaldehyde and acetaldehyde, can undergo chemical reactions in the atmosphere and form secondary pollutants in addition to their direct emissions into the atmosphere. Atmospheric oxidants play an important role in secondary toxics formation.

These oxidants are essentially the products of ozone chemistry. Therefore, it was necessary to carry out ozone-chemistry simulations during the toxics simulations. The ozone chemistry used in CAMx was the Statewide Air Pollution Research Center version 99 chemical mechanism (SAPRC99). The initial and boundary conditions for carrying out the ozone part of the simulation were taken from the 2000 Central California Ozone (CCOS) modeling.

To meet the CARE program's objectives, two sets of toxics simulations were performed: 1) with diesel particulate matter emissions only and 2) with full toxics species emissions.

3.2.1 Diesel Particulate Matter Modeling

Particulate matter emissions from all diesel sources in the Bay Area were included in this simulation. The eastern and northern boundary conditions from the surface to 500 m were set to 1 $\mu\text{g}/\text{m}^3$ and 0.5 $\mu\text{g}/\text{m}^3$ of PM concentrations, respectively, the average concentrations estimated from observations. Above 500 m, the boundary conditions were set to zero. The western and southern boundary conditions were set to zero from the surface to the top of the modeling domain. The initial conditions for interior model cells were also zero. With these specifications, the non-zero boundary conditions allowed pollutant penetration to the modeling domain when winds were from the east or from the north along the eastern or northern boundaries, respectively.

July 12-18 and December 12-18, 2000 were simulated. First, average diesel PM concentrations were calculated separately for the simulated July and December periods. Then an annual average concentration was calculated as 96% of the average of these two periods. The 96% factor was determined by comparing July and December observed CO average concentrations to annual average CO concentrations (See Appendix E for details).

Figures 1-3 show the distribution of simulated annual average PM concentrations as well as average concentrations for the simulated July and December periods. The highest annual average concentration was located over West Oakland (10-12 $\mu\text{g}/\text{m}^3$), extending toward Emeryville and along both sides of the eastern span of the Bay Bridge. The second highest concentrations (8-10 $\mu\text{g}/\text{m}^3$) were over Alameda, south-east of downtown Oakland, and the Transbay District/Rincon Hill areas in San Francisco. Several grid cells with concentrations ranging from 4 to 8 $\mu\text{g}/\text{m}^3$ exist just outside of these regions. Concentrations from 2 to 4 $\mu\text{g}/\text{m}^3$ cover an area from the Berkeley Marina in the north to San Leandro in the south and from downtown San Francisco in the west to Piedmont in the east. Areas just north and east of downtown San Jose also have an annual average concentration of 2-4 $\mu\text{g}/\text{m}^3$. Concentrations from 1 to 2 $\mu\text{g}/\text{m}^3$ cover an area from Richmond in the north to San Jose in the south and from San Francisco in the west to Piedmont in the east, mostly around freeways. Similar concentrations were estimated along portions of SR-4, I580 and I-680, as shown in the figure.

The highest summertime concentrations (4-6 $\mu\text{g}/\text{m}^3$) were located over areas of Oakland, Emeryville, and downtown San Francisco. Concentrations mainly to the east of the highest areas were 2-4 $\mu\text{g}/\text{m}^3$, falling to 1-2 $\mu\text{g}/\text{m}^3$. Outside of these areas, concentrations were below 1 $\mu\text{g}/\text{m}^3$. The reason summertime concentrations are significantly lower than the annual average is that during the afternoon hours of summer days, a strong sea breeze develops and allows pollutants to mix in the atmosphere. During the summer, the simulated high ambient toxics concentrations are, in general, toward the east of high emission areas because of predominant westerly winds. Airflow also splits over West Oakland, one branch continues toward Berkeley and the other toward San Leandro.

Wintertime concentrations however, were generally larger than the annual average concentrations over the core Bay Area. The maximum wintertime concentrations reached 16-18 $\mu\text{g}/\text{m}^3$ in West Oakland. Concentrations dropped sharply along the edges of the maximum area. Concentrations were 2-4 $\mu\text{g}/\text{m}^3$ over an area from Richmond in the north to San Jose in the south and from San Francisco in the west to the East Bay Hills in the east. These relatively high winter concentrations are mostly due to the stagnant meteorological conditions. Concentrations were 1-2 $\mu\text{g}/\text{m}^3$ over the entire Bay and its surrounding areas.

3.2.2 Full Toxics Modeling

The full chemistry toxics simulations included toxic compounds that were identified as significant contributors to the risk-weighted emissions in the Bay Area. The initial and boundary conditions were set to a small number, but greater than zero to avoid potential numerical problems. The full chemistry run was conducted for the same July 12-18 and December 12-18 periods as were modeled for the diesel PM only runs. The selected days were average summer and winter days from the meteorological perspective; however, December 2000 was, in general, an above average PM month. Additionally, PM concentrations in mid December are generally higher than other winter periods. Therefore, the simulated toxics concentrations were expected to represent high end winter concentrations.

Figures 4-18 show the annual average as well as monthly average concentrations for the simulated July and December periods for five toxics species (formaldehyde, acetaldehyde, benzene, 1,3-butadiene, acrolein). Again, the annual average concentrations are assumed to be 0.96 percent of the average July and December period concentrations. In the figures, the total concentrations are shown for species having both primary and secondary components.

The highest annual average formaldehyde concentrations were located at Travis Air Force Base in Fairfield (3-4.5 $\mu\text{g}/\text{m}^3$) and the San Francisco International Airport (3-5 $\mu\text{g}/\text{m}^3$) as shown in Figure 4. Concentrations in downtown San Francisco and San Jose reached 3-3.5 $\mu\text{g}/\text{m}^3$. Concentrations were 1-2.5 $\mu\text{g}/\text{m}^3$ in Oakland, Alameda, and parts of San Francisco and San Jose.

During the summer, the highest formaldehyde concentrations (1-2.5 $\mu\text{g}/\text{m}^3$) were located at Travis Air Force Base, the San Francisco International Airport, and downtown San Jose. Downtown San Francisco had formaldehyde concentrations ranging from 1-2 $\mu\text{g}/\text{m}^3$.

The distribution of wintertime formaldehyde concentrations is shown in Figure 6. The magnitude of wintertime concentrations was higher than the annual average concentrations. The winter average concentrations reached 8 $\mu\text{g}/\text{m}^3$ at Travis Air Force Base, the San Francisco International Airport, and downtown San Jose. In West Oakland and downtown San Francisco, the maximum concentrations reached 5 $\mu\text{g}/\text{m}^3$, with concentrations of 1-2 $\mu\text{g}/\text{m}^3$ in surrounding areas. Concentrations around 1 $\mu\text{g}/\text{m}^3$ extended from Richmond in the north to San Jose in the south and from San Francisco in the west to East Bay Hills in the east, mostly following freeways such as US-101 and I-880.

The highest annual average acetaldehyde concentrations (3.5-4 $\mu\text{g}/\text{m}^3$), shown in Figure 7, were located in West Oakland and downtown San Francisco. In the western part of downtown San Francisco and over Oakland, concentrations ranged from 2-2.5 $\mu\text{g}/\text{m}^3$. In downtown San Jose, concentrations were 1-2 $\mu\text{g}/\text{m}^3$. Concentrations near 1 $\mu\text{g}/\text{m}^3$ covered the entire Bay and its surrounding areas as well as Santa Rosa, Travis Air Force Base, and portions of the SR-4, SR-24, I-80, US-101, I-580 and I-680 corridors.

The highest summertime acetaldehyde concentrations (about 2-2.5 $\mu\text{g}/\text{m}^3$) were located in downtown San Francisco (Figure 8). West Oakland had concentrations ranging up to 2 $\mu\text{g}/\text{m}^3$. Concentrations ranging from 0.5-1 $\mu\text{g}/\text{m}^3$ were located around Oakland, Berkeley, San Jose, San Francisco and Travis Air Force Base. These regions were surrounded by concentrations around 0.25-0.5 $\mu\text{g}/\text{m}^3$.

Acetaldehyde concentrations for winter (Figure 9) reached 5 $\mu\text{g}/\text{m}^3$ in downtown San Francisco and 3 $\mu\text{g}/\text{m}^3$ in Oakland. Concentrations ranging from 0.5-2 $\mu\text{g}/\text{m}^3$ covered an area from Vallejo in the north to San Jose in the south and from San Francisco in the west to the East Bay Hills in the east. Concentrations up to 1 $\mu\text{g}/\text{m}^3$ were found in Santa Rosa.

The simulated annual average as well as average summer and winter concentrations for benzene are shown in Figures 10-12, for 1,3-butadiene in Figures 13-15 and for acrolein in Figures 16-18.

4. Risk Evaluation

Cancer risk from five toxics species (diesel PM, 1,3-butadiene, benzene, formaldehyde, and acetaldehyde) was calculated over the entire modeling domain. For this preliminary set of simulations, other modeled carcinogenic toxics species—with generally lower concentrations and smaller unit risk factors—were not included in this calculation, but could be in future assessments. The unit risk factors for the above species were, respectively, 300,

170, 29, 6, and 2.7, expected excess cancer cases per million per $\mu\text{g}/\text{m}^3$; these risk values assume a 70-year lifetime exposure (OEHHA, 2002).

Cancer risk for each species above was calculated by multiplying their respective annual average concentrations with their unit risk factors and then summing the resulting values. The results were expressed as the number of expected cancer incidences per million people and plotted in Figure 19. West Oakland had the highest number of expected cancer incidences of around 3,000 per million. Downtown San Francisco was second with a number around 2,500 per million. Expected incidences in the range of 2,250 to 2,500 per million were located over an area extending from Emeryville in the north to Alameda in the south and from West Oakland in the west to the I-580 corridor in the east. Similar numbers were also found in downtown Oakland. The numbers ranging from 500 to 1000 in a million covered an area from Richmond in the north to San Jose in the south and from San Francisco in the west to the East Bay Hills in the east, with Oakland connected to San Jose along the I-880 corridor. The number of expected incidences ranging from 250 to 500 in a million cover much of the Bay and its surrounding areas as well as Santa Rosa, Travis Air Force Base, and portions of the SR-4, SR-24, I-80, I-580 and I-680 corridors.

The cancer risk numbers were used to estimate expected excess cancers from toxic air contaminants in Bay Area populations. This was done by multiplying the cancer risk number of each grid cell by the actual population of that cell and dividing the result by one million. The expected excess cancer incidences, assuming a 70-year lifetime exposure, are shown in Figure 20.

The spatial distribution of the population-adjusted expected incidences was similar to that of number of the cancer risk estimates (per million people). However, some shift in the distribution was evident, reflecting the Bay Area population densities. The highest number of population-adjusted incidences was around 40, occurring over a grid cell in downtown San Francisco. The second highest number of around 25 was also in downtown San Francisco, extending toward Civic Center. Population-adjusted expected incidences around 15 were found in east Oakland and west and south of the San Francisco Civic Center. Expected incidences around 10 were found in much of Oakland and a small portion of San Francisco. Incidences around 5 were found in an area from Richmond and San Francisco in the north to San Jose in the south, mostly following the major freeways.

The population-adjusted cancer incident numbers were also calculated using only “sensitive populations” defined here as people over 64 and under 18. The resulting distribution of expected incident numbers is displayed in Figure 21. The highest expected incident number was around 10, located over downtown Oakland and San Francisco. A value of around 5 covers much of downtown Oakland, downtown San Francisco, and a small portion of eastern San Jose.

5. Conclusion and Further Study

This study summarizes the Bay Area Air Quality Management District's modeling and analysis of regional-scale simulations of toxic air contaminants (TAC). The study represents a significant step forward for District modeling capabilities: for the first time, TAC modeling was performed at a regional scale. The study developed model-ready TAC emissions for 2005 to predict selected TAC concentrations for two seasons—a summer and a winter period—and estimated annual concentrations from some of these selected compounds. The compounds selected—diesel particulate matter (diesel PM), benzene, 1,3-butadiene, formaldehyde, acetaldehyde, and acrolein—were determined to be primary contributors to health risk, both cancer and non-cancer risk for the region.

One of the important findings of this study was that, many areas of the Bay Area have a cancer risk level of between 250 and 500 per million, based on unit cancer risk factors from the Office of Environmental Health Hazard Assessment (OEHHA; OEHHA, 2002). Highest areas in the District have risk levels greater than 1000. These risk levels are supported by observed risk-weighted TAC concentrations.

A second important finding is that, like risk-weighted TAC emissions, risk from TAC concentrations and TAC exposures are focused in several core urban areas of the region near major freeways, ports, and areas with high levels of construction. For the first time, we have estimates of TAC risk, at high spatial resolution, in the Bay Area.

The information brought to light through this modeling study suggests additional future work that could provide still more insight into the sources and nature of TAC concentrations in the Bay Area. For example, future studies could include more TAC species in the modeling and risk analyses. At a regional level, using health risk factors from the OEHHA, the compounds included in this study represent the most of the health risk from TAC in the Bay Area. However, it is very likely that there are localized areas where health effects of other compounds are important to consider in addition to the compounds included in this study.

In this work, as for all modeling studies, there was a trade-off between spatial resolution and the length of the simulations. In future work it would be useful to consider longer simulations, to include multiple weeks in a season and, perhaps, additional seasons to help refine the estimate of annual concentrations and annual risk.

This study provided modeling results to characterize risk levels representative of base conditions in 2005. Future modeling studies could address the influence and importance of specific source regions and source categories. For example, it would be helpful to see the contributions of stationary sources versus mobile sources to total risk. Moreover, it would be extremely informative to investigate the changes to the levels and distribution of risk in future years. Specifically, the California Air Resources Board (CARB) has recently adopted Air Toxic Control Measures (ACTMs) for diesel drayage trucks, on-road trucks, ships, and other sources that collectively were designed to reduce diesel emissions in California by 80% by 2020 relative to 2000 (CARB, 2000). Future year simulations that include these reductions

measures and reduction measure implemented by the Air District for stationary sources would help to evaluate risk-reduction benefits of these measures in the Bay Area.

6. References

- (CARB, 2000). "Risk Reduction Plan to Reduce Particulate Matter Emissions from Diesel-Fueled Engines and Vehicles," California Air Resources Board, Stationary Source Division Mobile Source Control Division. Available on-line at <http://www.arb.ca.gov/diesel/documents/rrpapp.htm>. October 2000.
- (ENVIRON, 2008). "Demonstration of Toxics Modeling for the Bay Area using CAMx," Final Report prepared by ENVIRON International Corporation for the Bay Area Air Quality Management District. February, 2008.
- (OEHHA, 2002). "Air Toxics Hot Spots Program Risk Assessment Guidelines, Part II, Technical Support Document for Describing Available Cancer Potency Factors," Office of Environmental Health Hazard Assessment. Available on-line at http://oehha.ca.gov/air/cancer_guide/TSD2.html. December 2002.
- (STI, 2006). "Preparation of Emission Inventories of Toxic Air Contaminants for the Bay Area," Final Report prepared by Sonoma Technology, Inc. for the Bay Area Air Quality Management District. STI-906020.07-2771-FR2. August, 2006.
- (STI, 2008). "Final documentation of the preparation of year-2005 emission inventories of toxic air contaminants for the San Francisco Bay Area," Final Report prepared by Sonoma Technology, Inc. for the Bay Area Air Quality Management District. STI-906020.08-3288. February, 2008.

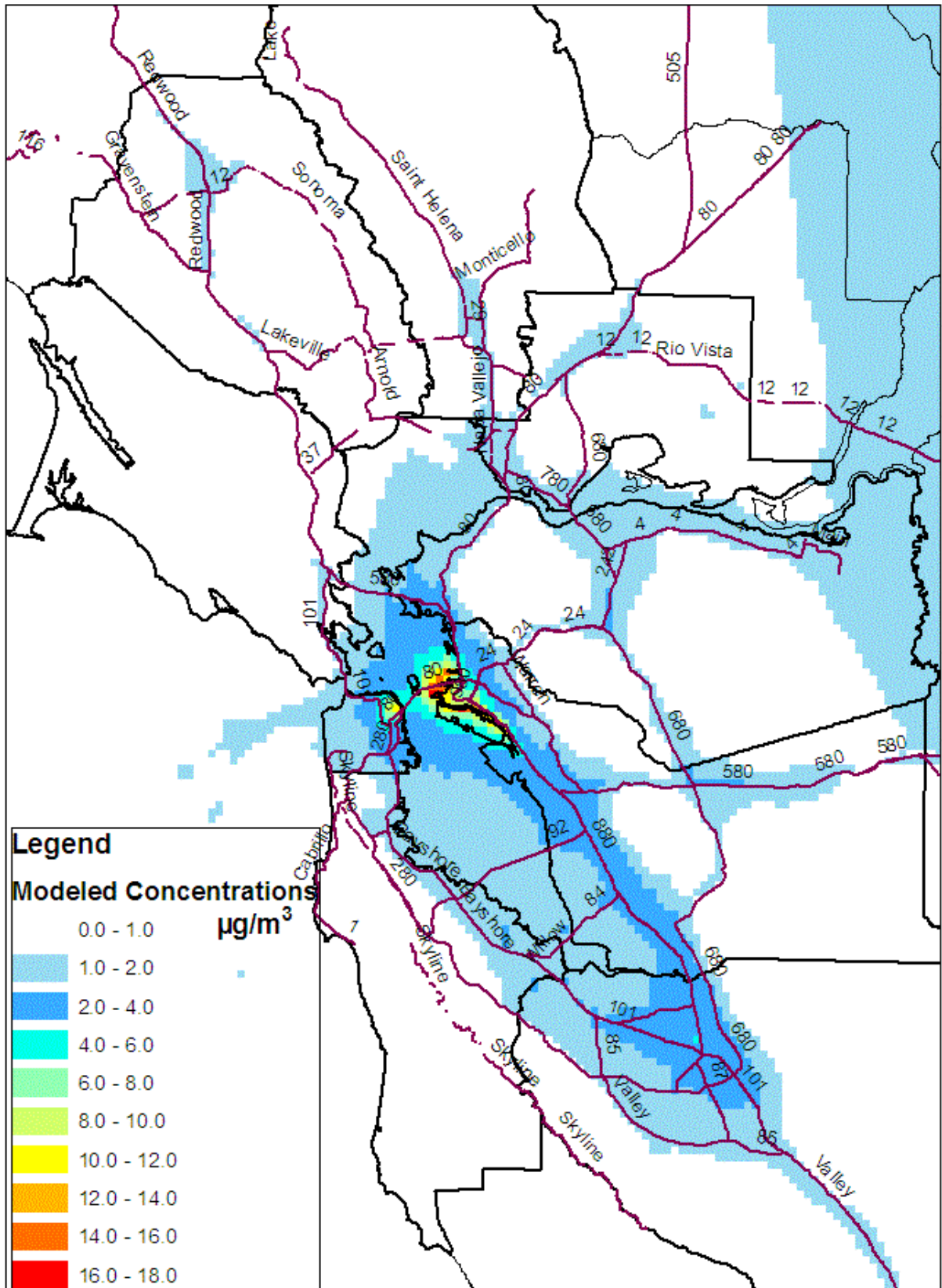


Figure 3: Diesel PM concentrations for December.

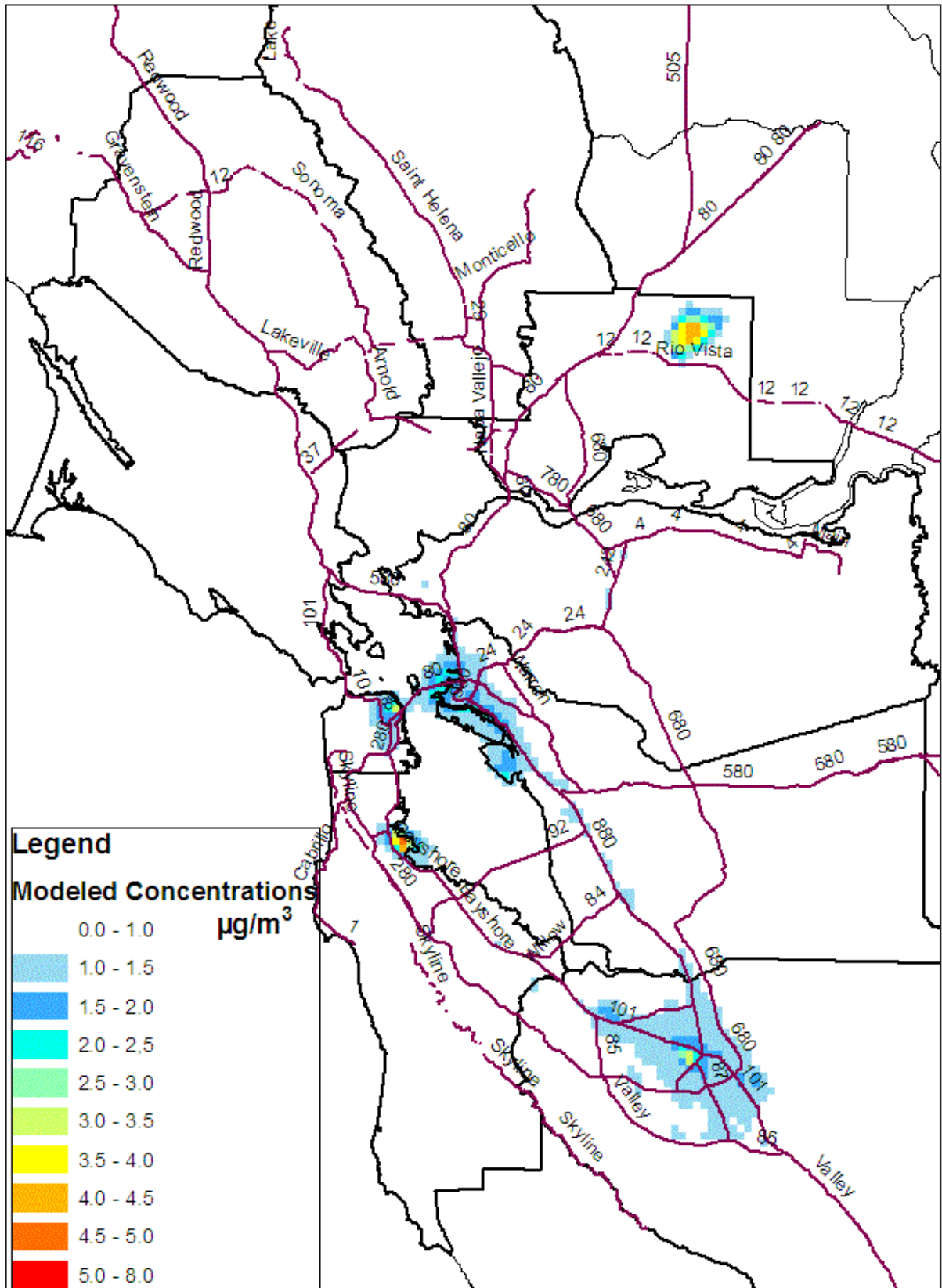


Figure 4: Annual average formaldehyde concentrations.

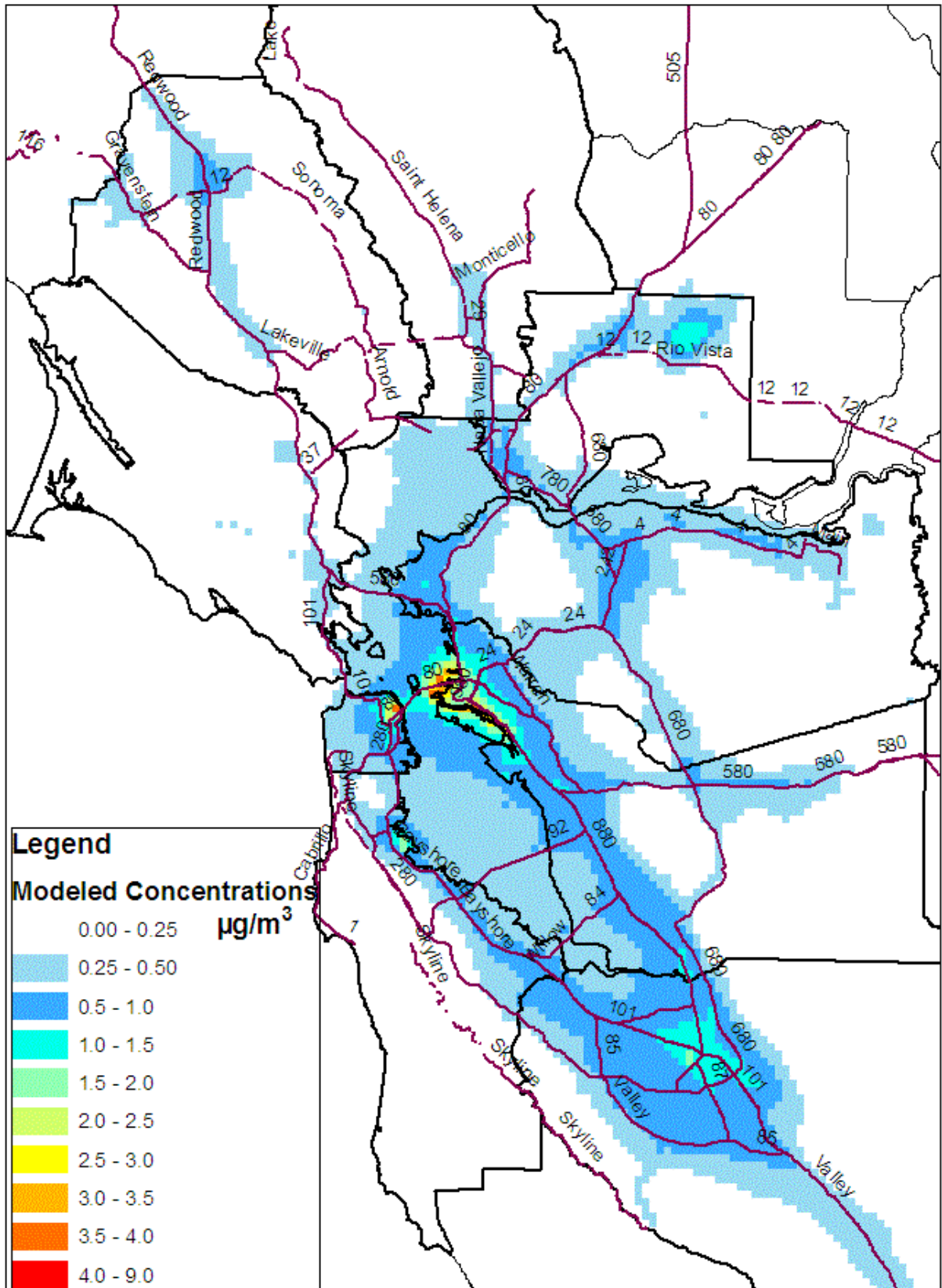


Figure 7: Annual average acetaldehyde concentrations.

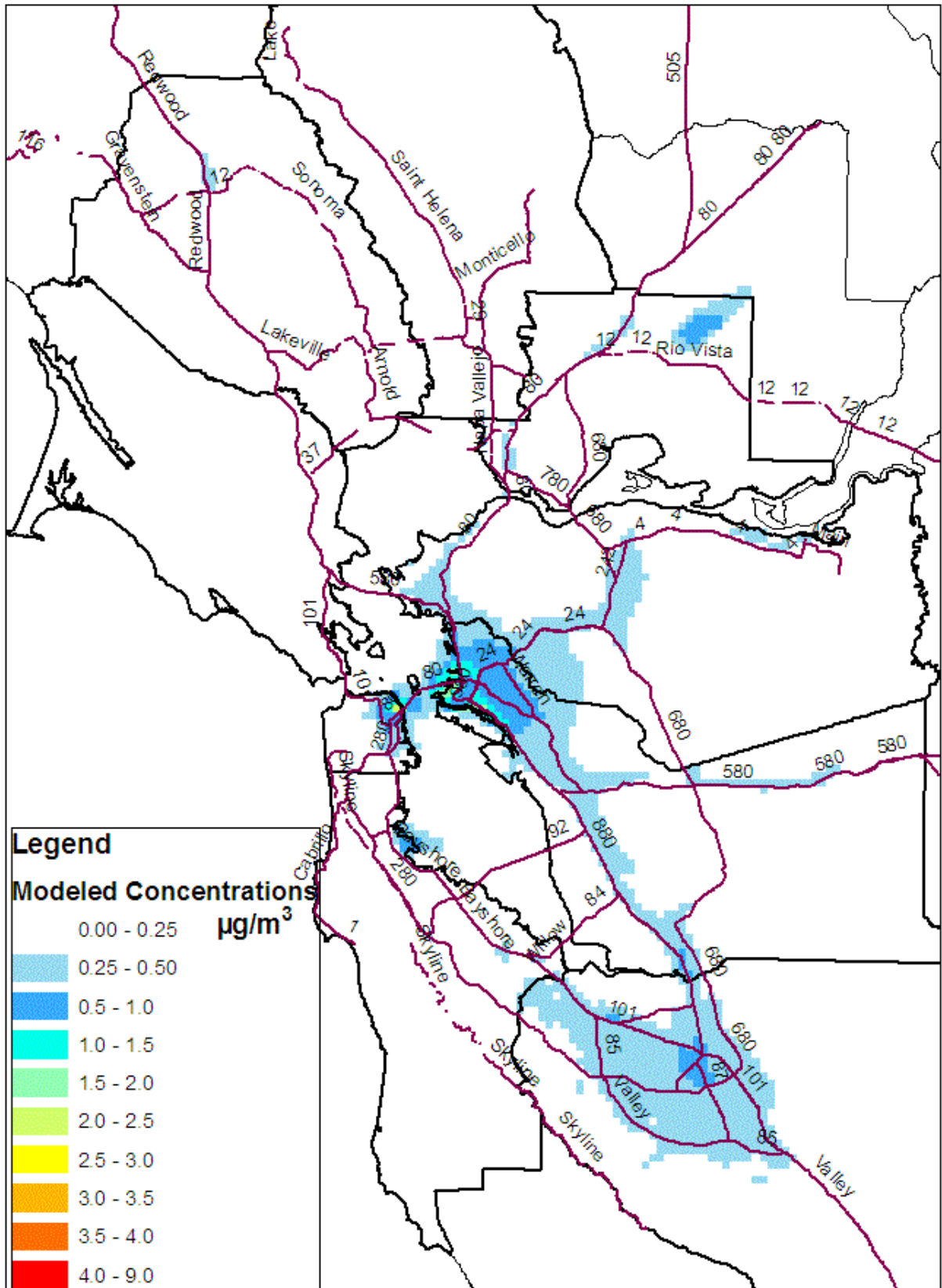


Figure 8: Acetaldehyde concentrations for July.

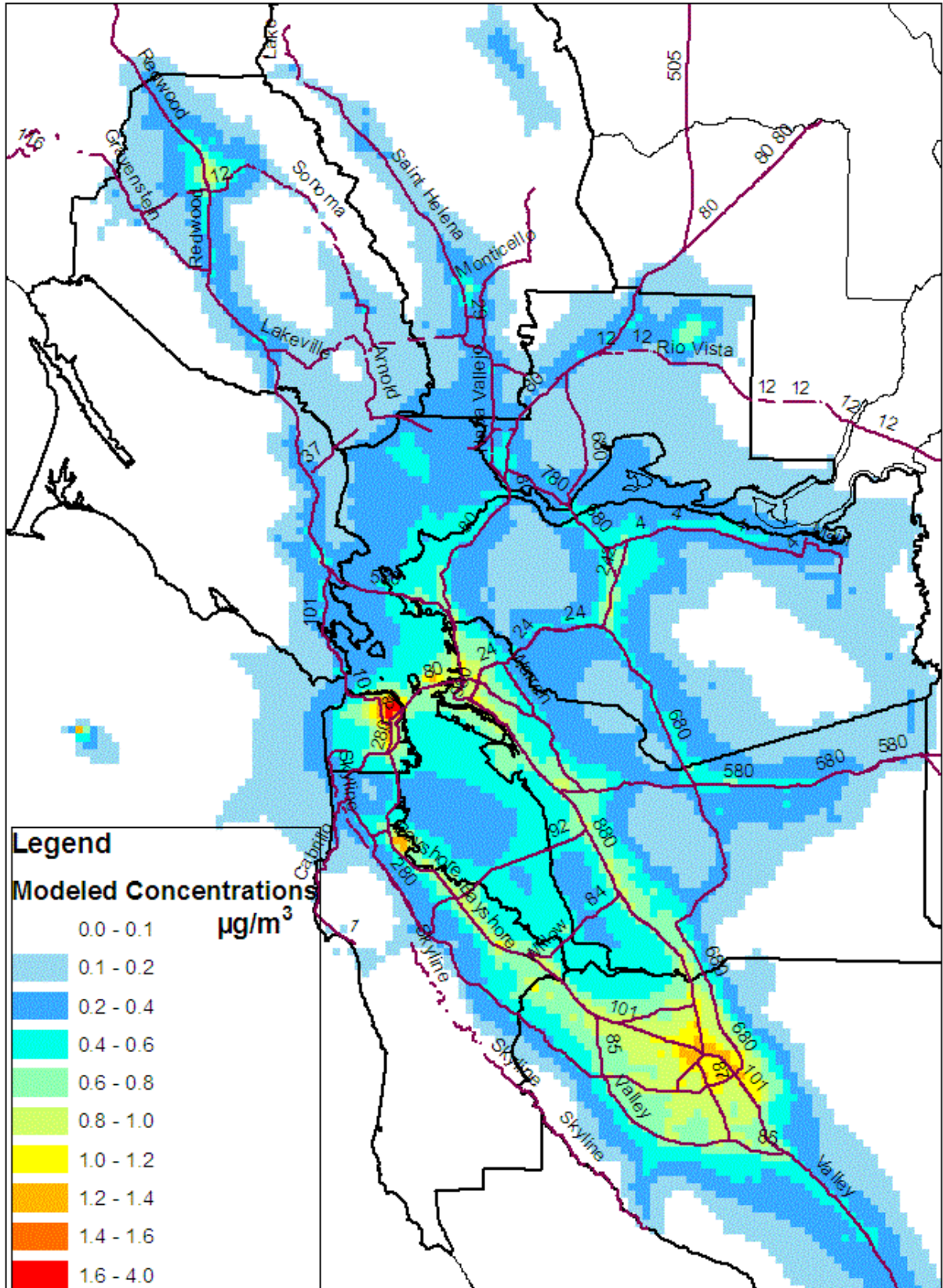


Figure 10: Annual average benzene concentrations.

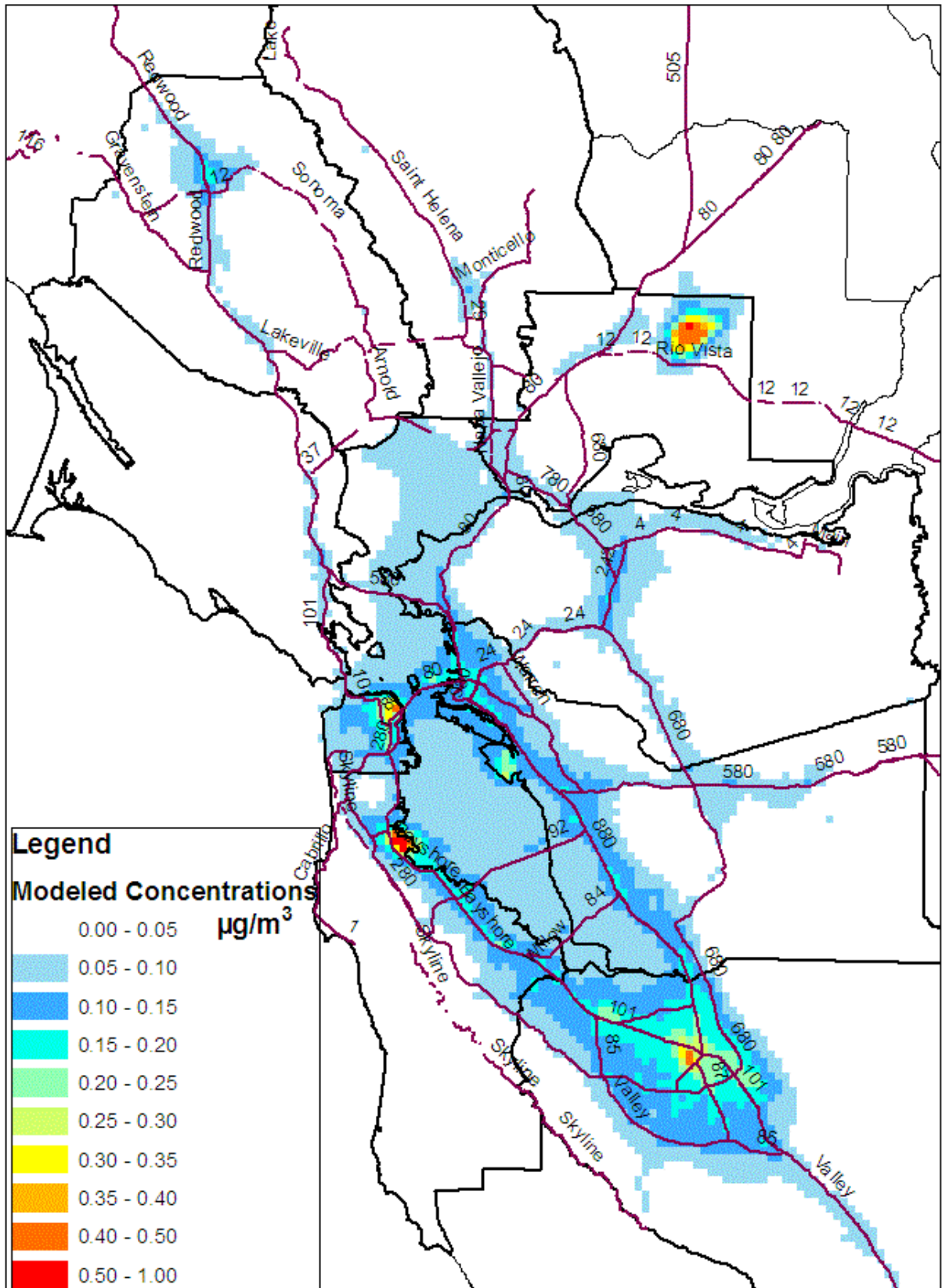


Figure 13: Annual average 1,3-butadiene concentrations.

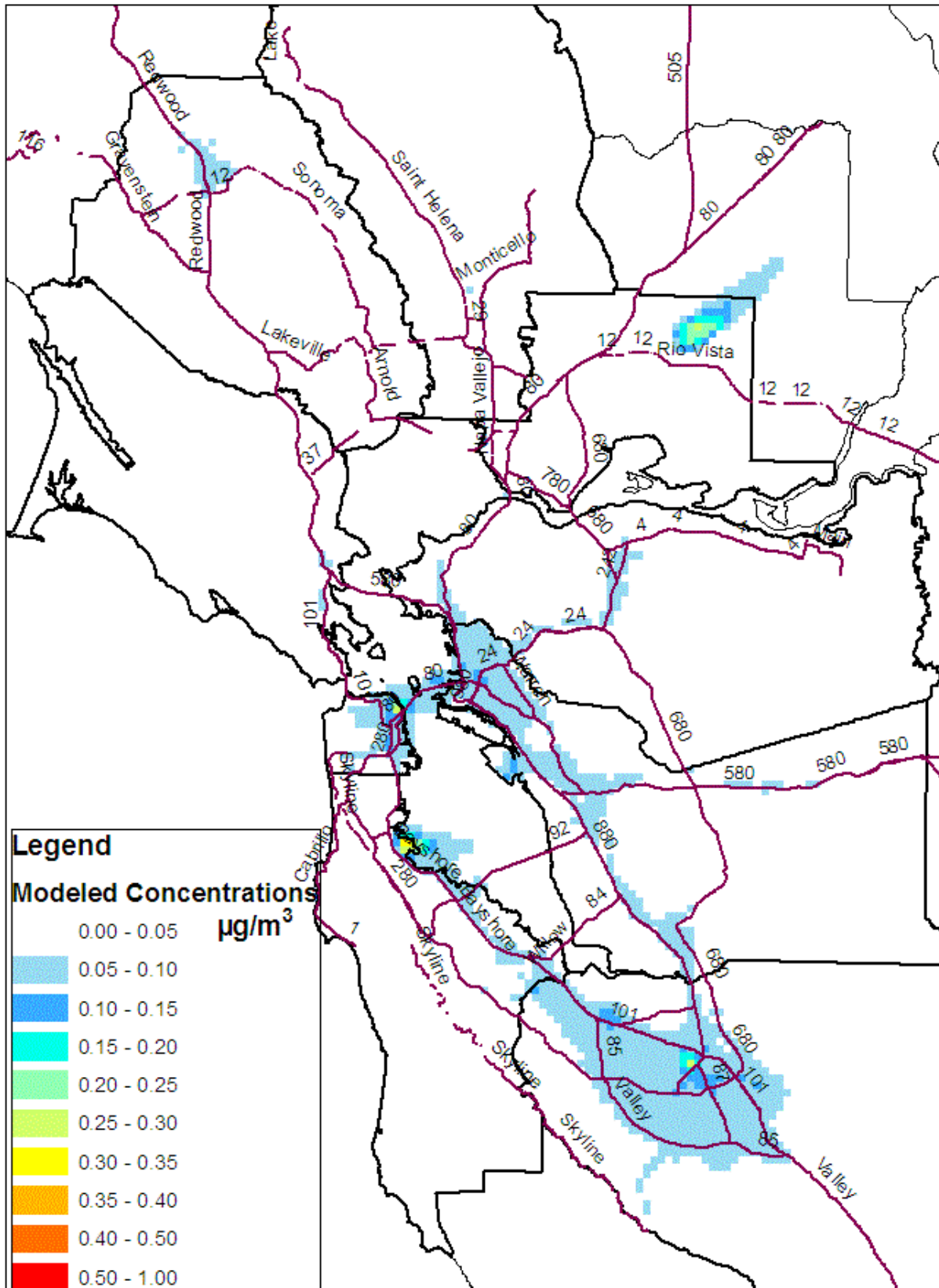


Figure 14: 1,3-butadiene concentrations for July.

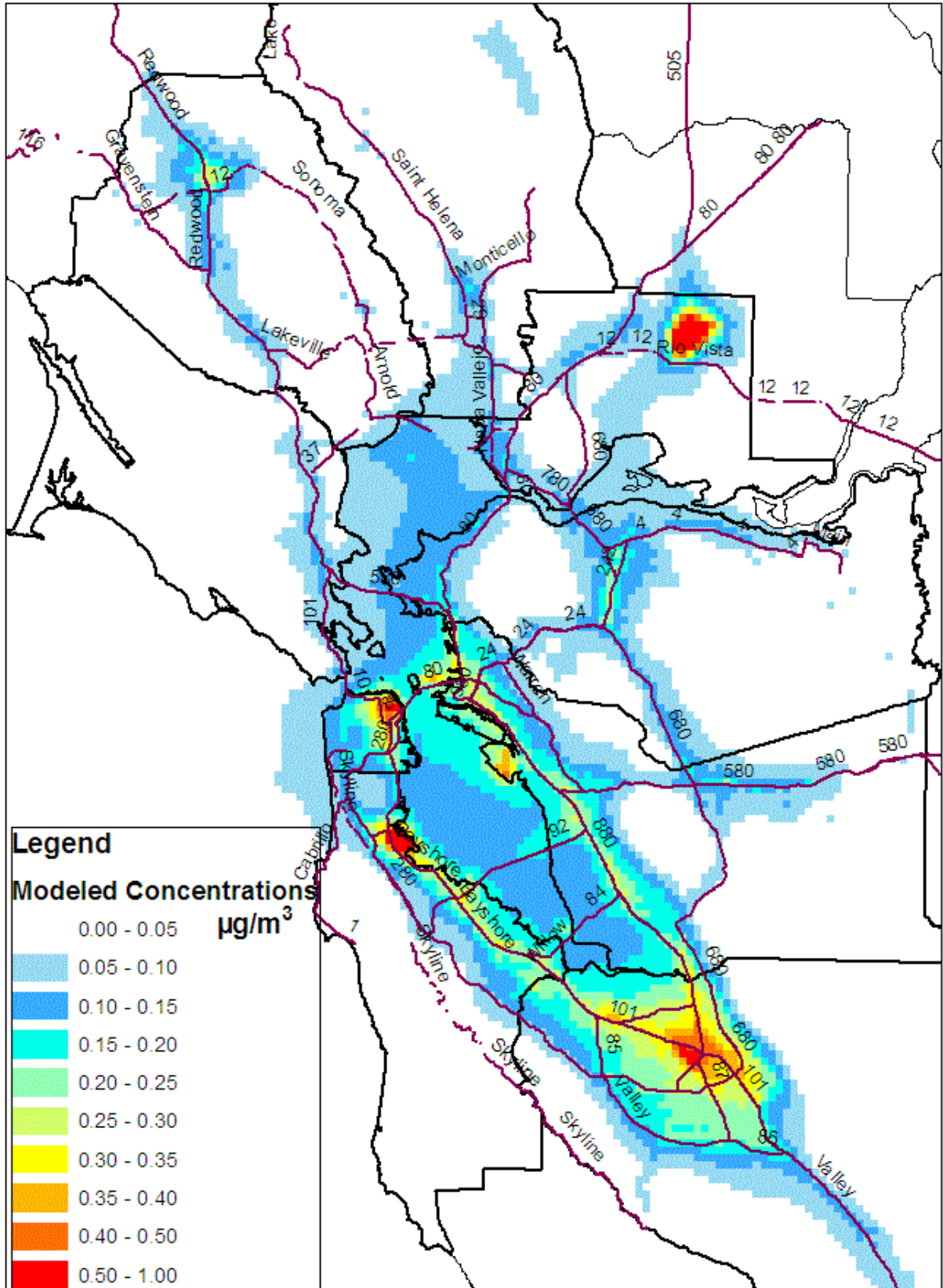


Figure 15: 1,3-butadiene concentrations for December.

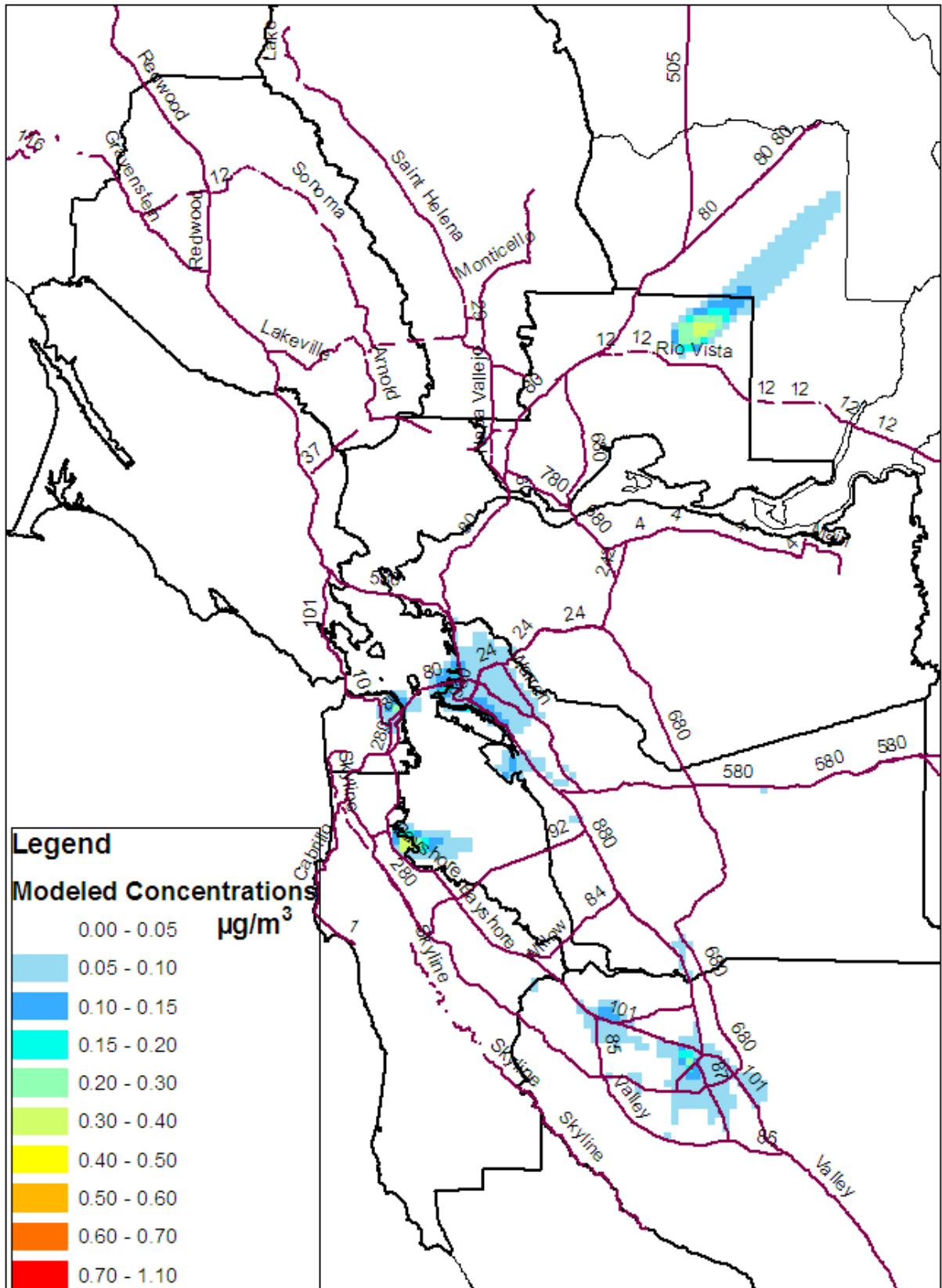


Figure 17: Acrolein concentrations for July.

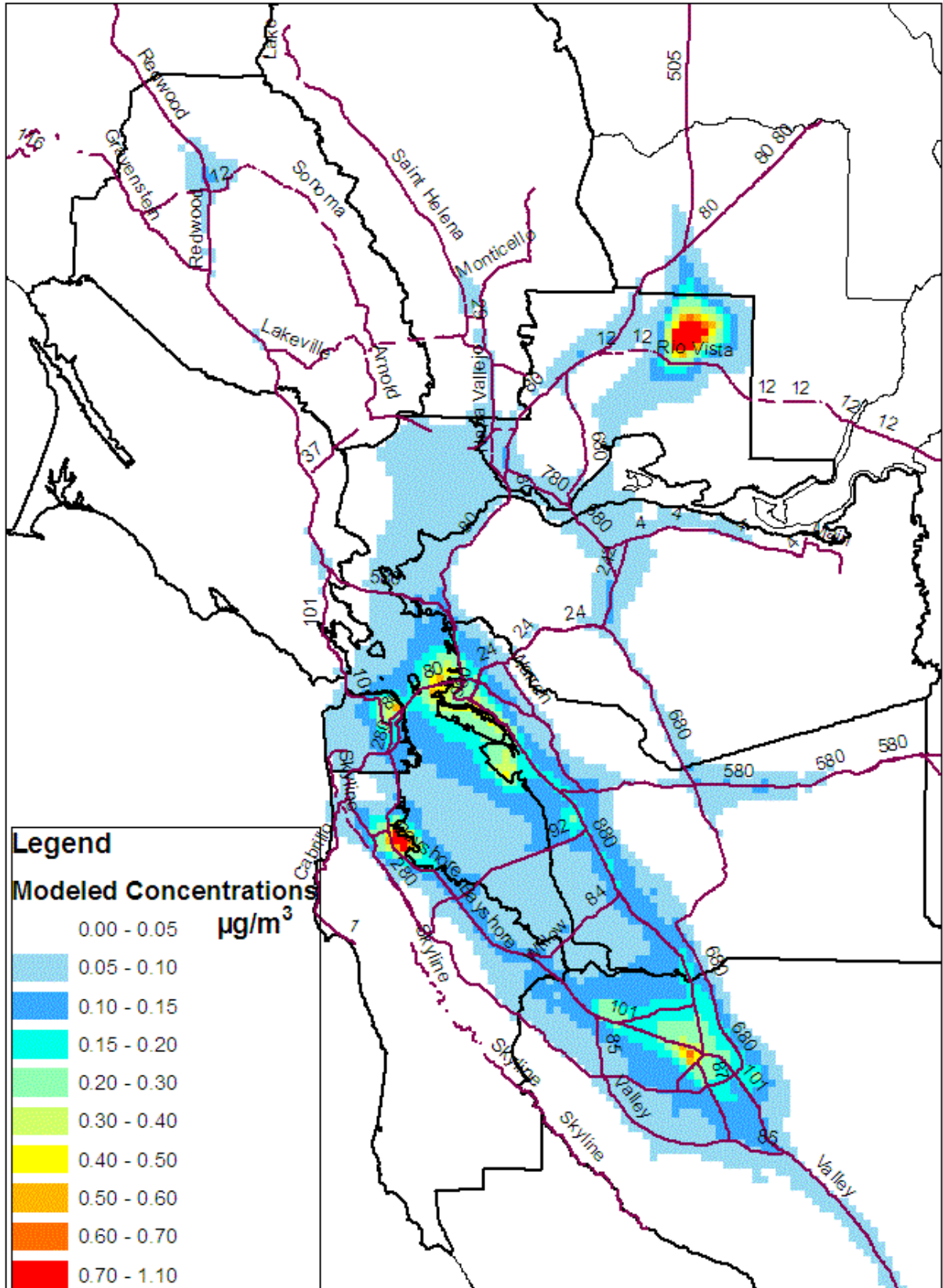


Figure 18: Acrolein concentrations for December.

APPENDIX A

Toxics Emissions Inventory

The following tables and figures give information on the magnitude and spatial distributions of emissions of key toxics species.

Table A1 summarizes 2005 diesel particulate matter of less than ten microns (DPM10) emissions by Bay Area county and major source category. Overall, area and non-road equipment emissions dominate, with Alameda and San Mateo Counties showing the two highest emission estimates.

Table A1: DPM10 emissions by county and major source category (tons/day).

County	Area/Non-road	On-road	Stationary Point	Total
Alameda	2.04	1.40	0.02	3.46
Contra Costa	0.81	0.51	0.05	1.37
Marin	0.36	0.09	0.00	0.45
Napa	0.11	0.10	0.00	0.21
San Francisco	1.22	0.19	0.01	1.42
San Mateo	1.92	0.20	0.01	2.13
Santa Clara	0.86	0.76	0.03	1.65
Solano	0.26	0.26	0.01	0.53
Sonoma	0.25	0.19	0.01	0.45
Grand Total	7.83	3.70	0.14	11.67

Note: Emissions from diesel off-road categories estimated in ARB's OFFROAD model have been halved based on District staff's fuel-based analysis.

Table A2 shows detailed contributions to the area/non-road DPM10 emissions by county from Table A1. These two tables show that ship emissions are the largest source of DPM10 for Marin, San Francisco, and San Mateo Counties, while they are second only to on-road sources in Alameda County. Construction equipment (included under off-road equipment in Table A2) is a significant source for the majority of counties.

Tables A3-A7 show 2005 county-level emissions of acetaldehyde, acrolein, 1,3-butadiene, formaldehyde and benzene, respectively. Emissions are broken out by major source category.

Table A2: Area and non-road DPM10 emissions by county (tons/day).

COUNTY	FARM EQUIPMENT	MANUFACTURING AND INDUSTRIAL	OFF-ROAD EQUIPMENT	RECREATIONAL BOATS	SHIPS AND COMMERCIAL BOATS	TRAINS	Grand Total
Alameda	0.02	0.02	0.63	0.0002	1.28	0.09	2.04
Contra Costa	0.02	0.01	0.47	0.0007	0.21	0.09	0.80
Marin	0.01	0.00	0.10	0.0002	0.24	0.00	0.35
Napa	0.04	0.00	0.05	0.0004		0.02	0.11
San Francisco	0.00	0.02	0.44	0.0002	0.73	0.03	1.22
San Mateo	0.01	0.01	0.28	0.0001	1.59	0.03	1.92
Santa Clara	0.04	0.03	0.70	0.0004		0.08	0.85
Solano	0.04	0.00	0.12	0.0001	0.07	0.02	0.25
Sonoma	0.04	0.01	0.18	0.0002	0.01	0.02	0.26
Grand Total	0.22	0.10	2.97	0.0025	4.13	0.38	7.80

Table A3: Acetaldehyde emissions by county and major source category (lbs/day).

County	Area/Non-road	On-road	Point	Total
Alameda	1953	1119	1.4	3073
Contra Costa	1184	477	3.2	1664
Marin	350	100	0.0	450
Napa	229	99	0.0	328
San Francisco	658	180	0.0	838
San Mateo	674	213	0.0	887
Santa Clara	1359	697	20.7	2077
Solano	648	397	0.8	1046
Sonoma	560	198	10.1	768
Grand Total	7615	3480	36	11131

Note: Emissions from diesel off-road categories estimated in ARB's OFFROAD model have been halved based on District staff's fuel-based analysis.

Table A4: Acrolein emissions by county and major source category (lbs/day).

County	Area/Non-road	On-road	Point	Total
Alameda	179	128	0.6	308
Contra Costa	75	65	0.0	140
Marin	24	15		39
Napa	22	14	0.0	36
San Francisco	59	29	0.0	88
San Mateo	113	37		150
Santa Clara	130	99		229
Solano	193	41		234
Sonoma	33	31		64
Grand Total	828	459	1	1288

Note: Emissions from diesel off-road categories estimated in ARB's OFFROAD model have been halved based on District staff's fuel-based analysis.

Table A5: 1,3-butadiene emissions by county and major source category (lbs/day).

County	Area/Non-road	On-road	Point	Total
Alameda	225	283	0.0	508
Contra Costa	106	197	3.5	307
Marin	64	52		116
Napa	39	43		82
San Francisco	65	104		169
San Mateo	121	142		263
Santa Clara	132	314	0.2	446
Solano	168	64	0.3	232
Sonoma	41	112		153
Grand Total	961	1311	4	2276

Note: Emissions from diesel off-road categories estimated in ARB's OFFROAD model have been halved based on District staff's fuel-based analysis.

Table A6: Formaldehyde emissions by county and major source category (lbs/day).

County	Area/Non-road	On-road	Point	Total
Alameda	1655	1203	35	2893
Contra Costa	1329	688	358	2375
Marin	475	165	1	641
Napa	284	150	8	442
San Francisco	606	318	48	972
San Mateo	1044	428	15	1487
Santa Clara	1523	1053	181	2757
Solano	1441	352	13	1806
Sonoma	586	351	2	939
Grand Total	8943	4708	661	14312

Note: Emissions from diesel off-road categories estimated in ARB's OFFROAD model have been halved based on District staff's fuel-based analysis.

Table A7: Benzene emissions by county and major source category (lbs/day).

County	Area/Non-road	On-road	Point	Total
Alameda	639	1362	10	2011
Contra Costa	617	935	148	1701
Marin	294	250	1	546
Napa	175	203	1	379
San Francisco	373	498	2	872
San Mateo	444	675	4	1124
Santa Clara	651	1516	46	2212
Solano	334	301	8	643
Sonoma	205	527	3	735
Grand Total	3733	6268	223	10224

Note: Emissions from diesel off-road categories estimated in ARB's OFFROAD model have been halved based on District staff's fuel-based analysis.

Table A8 shows Bay Area county-level total organic gas (TOG) and nitrogen oxides (NOx) by major source category.

Table A8: 2005 Bay Area annual average TOG and NOx emissions by county and major source category (tons/day).

County	TOG						NOx					Total
	Point	Area	On-road	Non-road	Natural	Total	Point	Area	On-road	Non-road	Natural	
Alameda	106.4	32.7	33.4	16.5	12.2	201.2	5.3	3.9	65.6	46.1	0.1	121.0
Contra Costa	96.2	24.5	22.5	11.8	12.1	167.1	21.2	2.9	34.4	18.6	0	77.1
Marin	21	14.4	6.2	5.7	7.7	55.0	0.4	1	8.8	6.1	0.1	16.4
Napa	14.9	10.7	4.9	3.4	31.4	65.3	0.6	0.4	6.8	2.6	1.2	11.6
San Francisco	13.1	14.2	12.2	8.7	1	49.2	3.1	2.5	18	22.0	-	45.6
San Mateo	43.5	14.5	15.9	9.8	7.4	91.1	1.5	2.3	20.8	41.2	-	65.8
Santa Clara	147.8	35.2	37.4	15.8	31.1	267.3	9.7	4.6	52.4	23.8	0.2	90.7
Solano	17.6	6.4	6.3	6.7	2.7	39.7	6.3	0.7	11.7	8.1	-	26.8
Sonoma	26.1	21	12.1	4.7	10.6	74.5	0.5	1.2	15.3	5.5	0	22.5
Total	486.6	173.6	150.9	83.1	116.2	1010.4	48.6	19.5	233.8	174.2	1.6	477.7

Source: ARB's planning emissions inventory at <http://www.arb.ca.gov/app/emsmv/emssumcat.php>.

Note: Emissions from diesel off-road categories estimated in ARB's OFFROAD model have been halved based on District staff's fuel-based analysis.

Figure A1 illustrates the Bay Area-wide hourly distribution of DPM10 emissions for a weekday and weekend day. It clearly shows a drop in overall activity on weekend days. Since ship, construction equipment, and heavy-duty truck emissions dominate for this pollutant, most of the emissions occur during daylight hours. Note that stationary point source emissions are not included in the figure. Overall, these are small contributions that tend to be flat throughout the day.

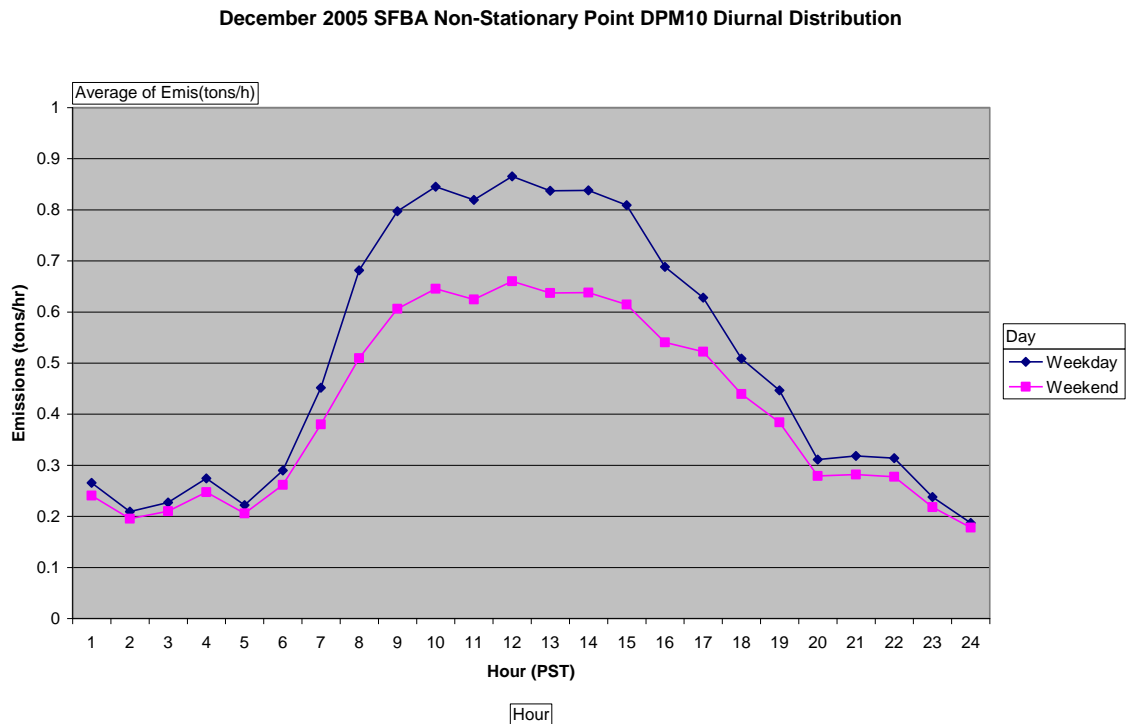


Figure A1: December weekday and weekend day diurnal distributions of DPM10 emissions (emissions from stationary point sources are not included).

The following plots give general spatial distributions of DPM10, formaldehyde, acetaldehyde, 1,3-butadiene, acrolein and benzene emissions. As discussed above, DPM10 originates mostly from ships, construction equipment, and heavy-duty trucks and is shown below to be concentrated in areas where these activities occur (shipping lanes, populated areas, and major highways). Formaldehyde, acetaldehyde, 1,3-butadiene, acrolein and benzene are generally combustion byproducts. In particular, aircraft are a significant source of acrolein so that emissions of acrolein are concentrated around large airfields. Benzene is emitted primarily in the exhaust of combustion engines and through gasoline evaporation; therefore, its emissions follow the major roadways and are found in the populated areas.

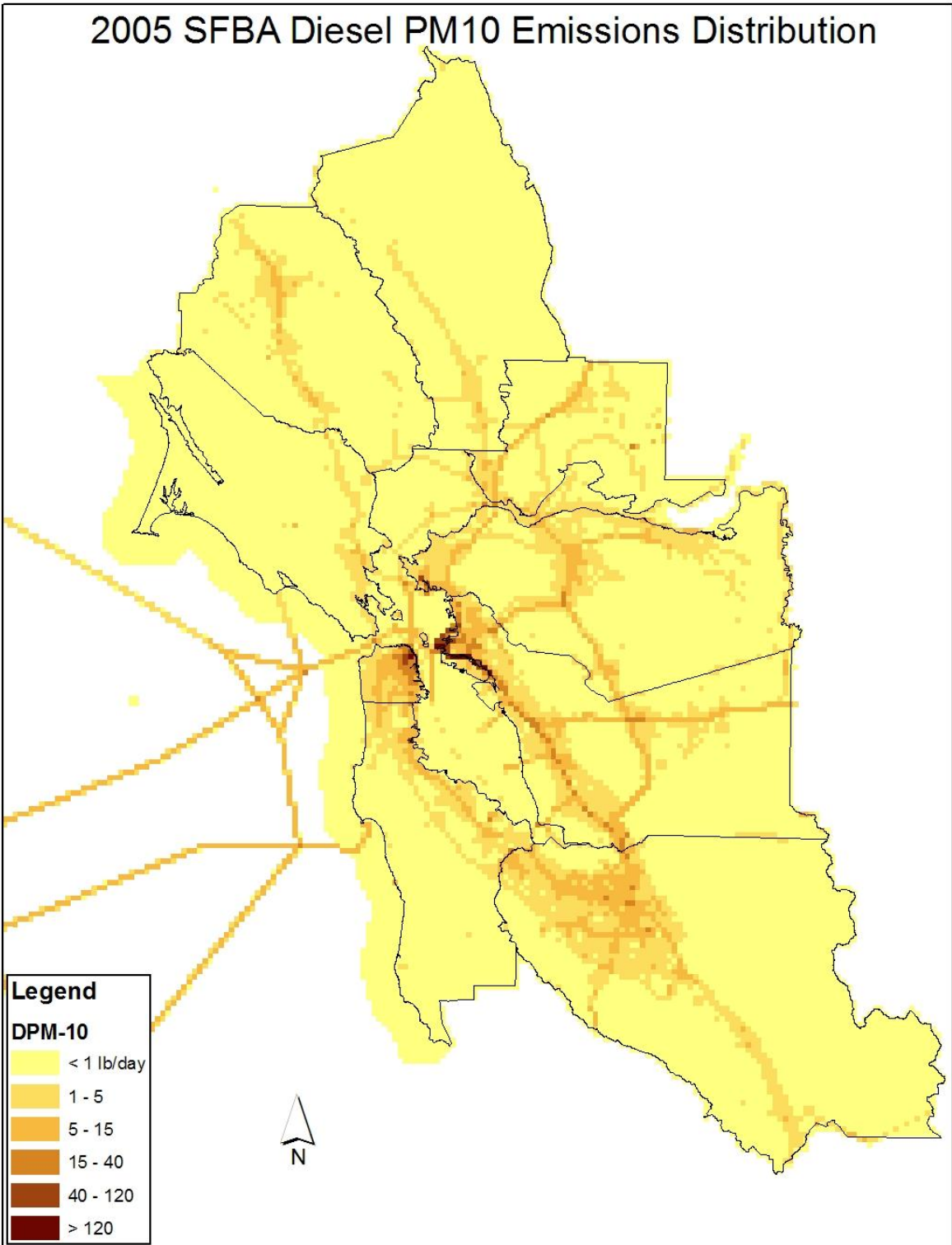


Figure A2: Spatial distribution of DPM10 emissions in the Bay Area.

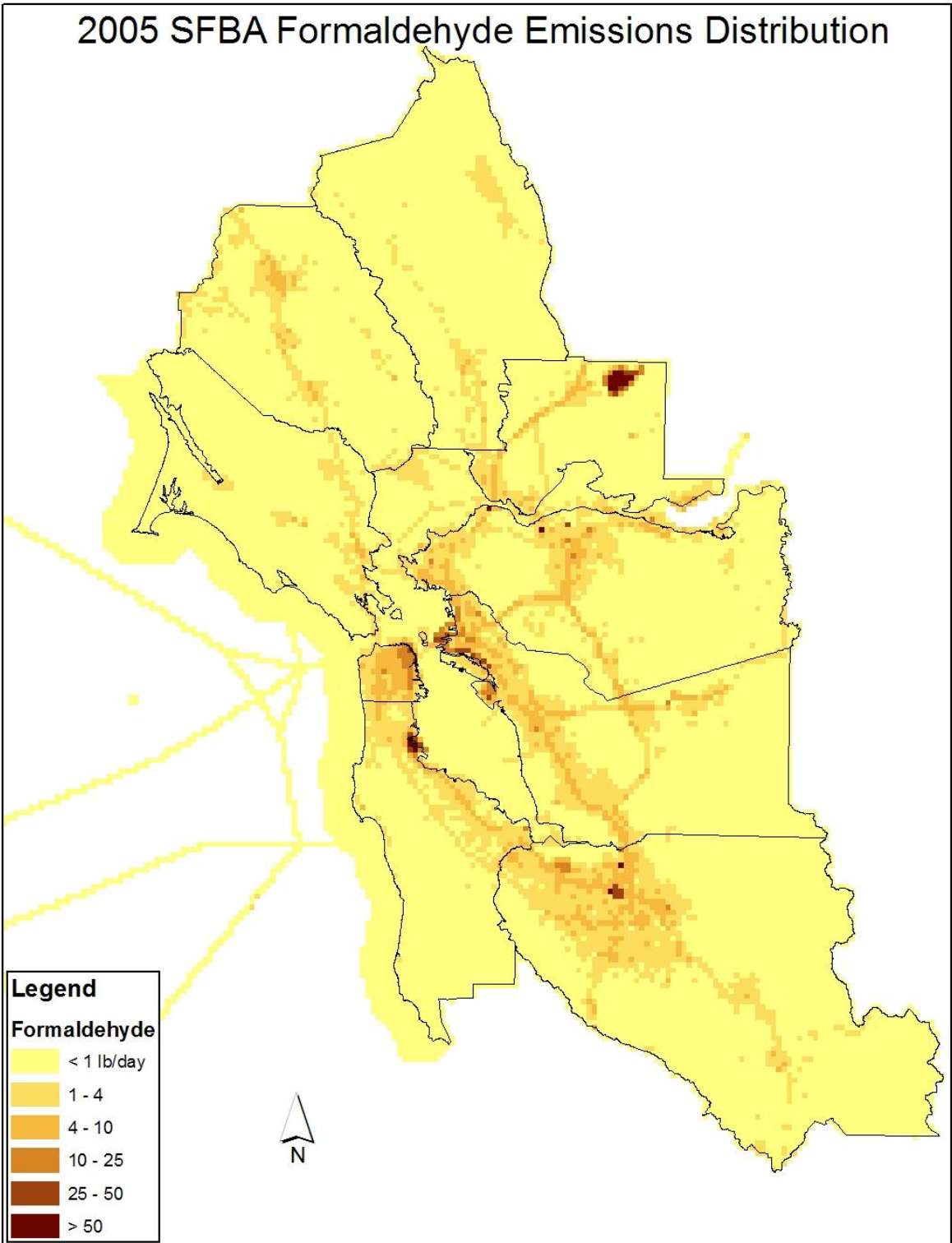


Figure A3: Spatial distribution of formaldehyde emissions in the Bay Area.

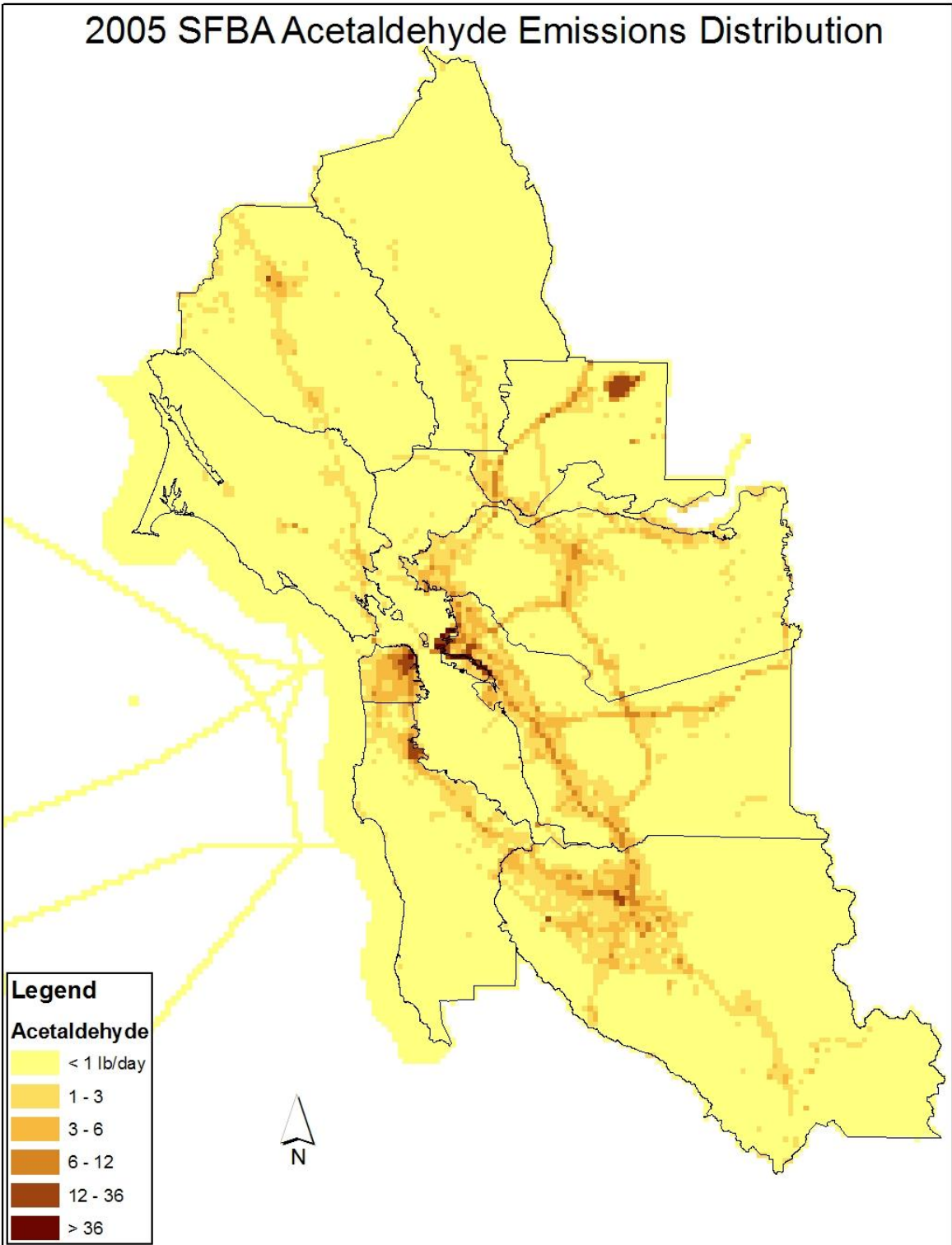


Figure A4: Spatial distribution of acetaldehyde emissions in the Bay Area.

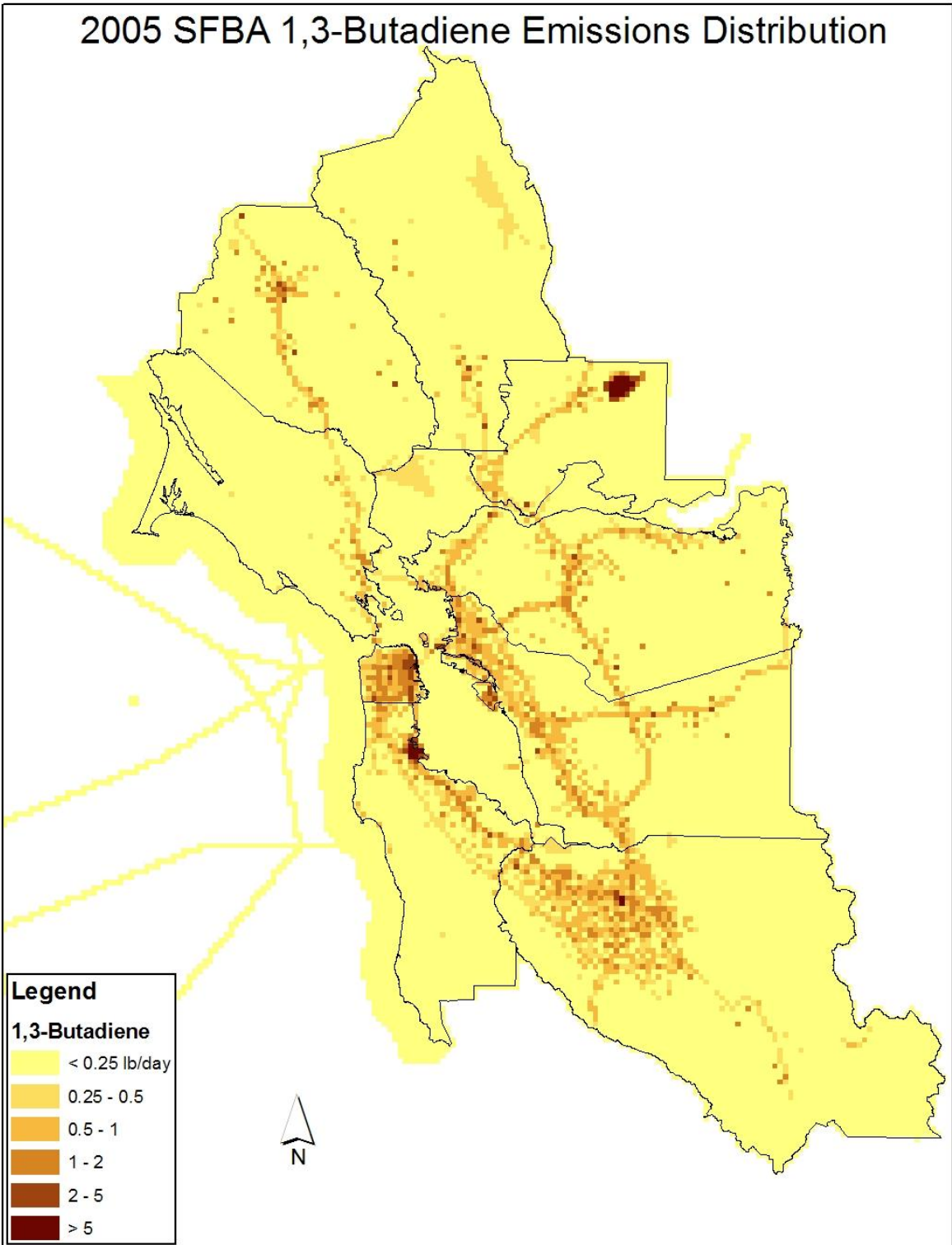


Figure A5: Spatial distribution of 1,3-butadiene emissions in the Bay Area.

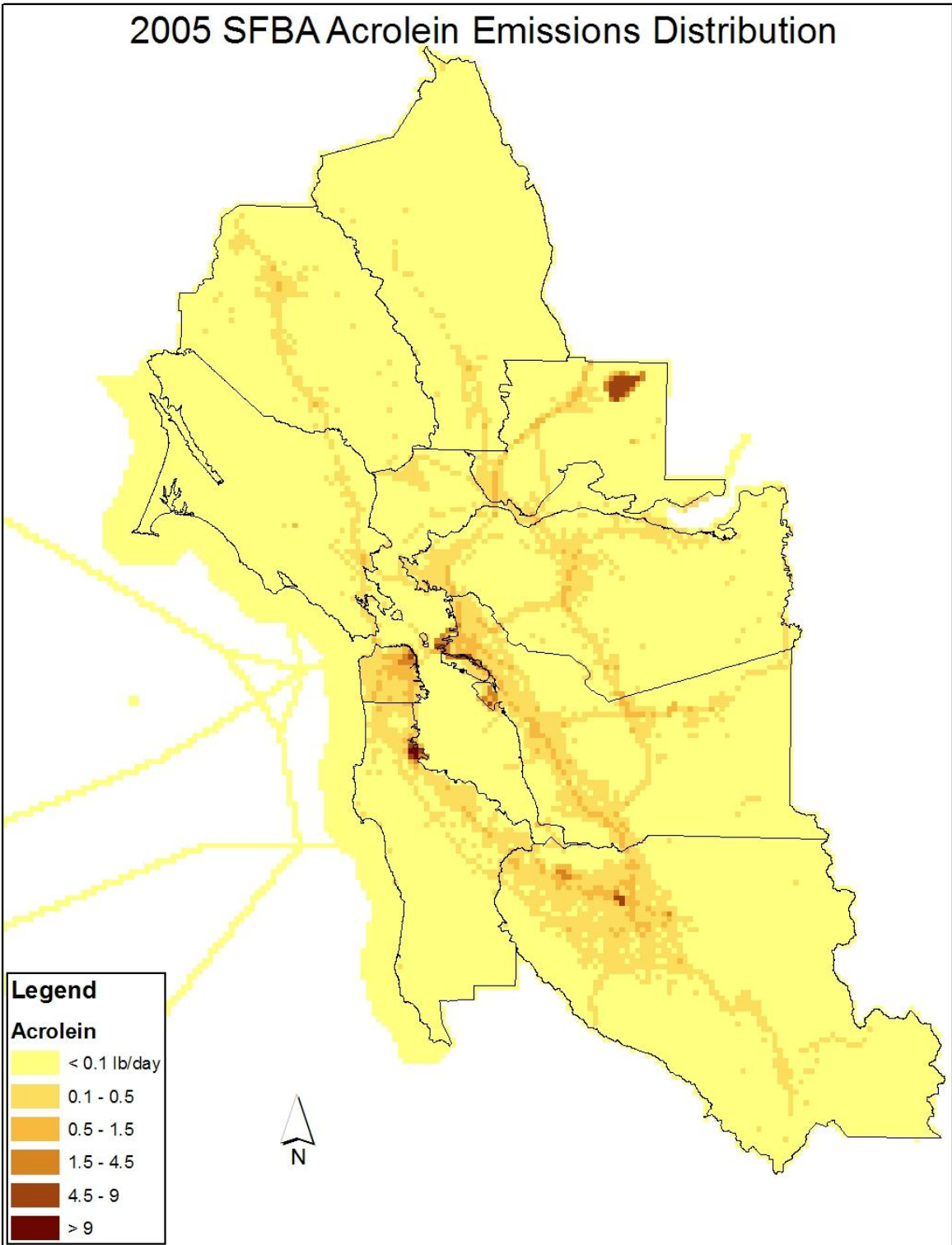


Figure A6: Spatial distribution of acrolein emissions in the Bay Area.

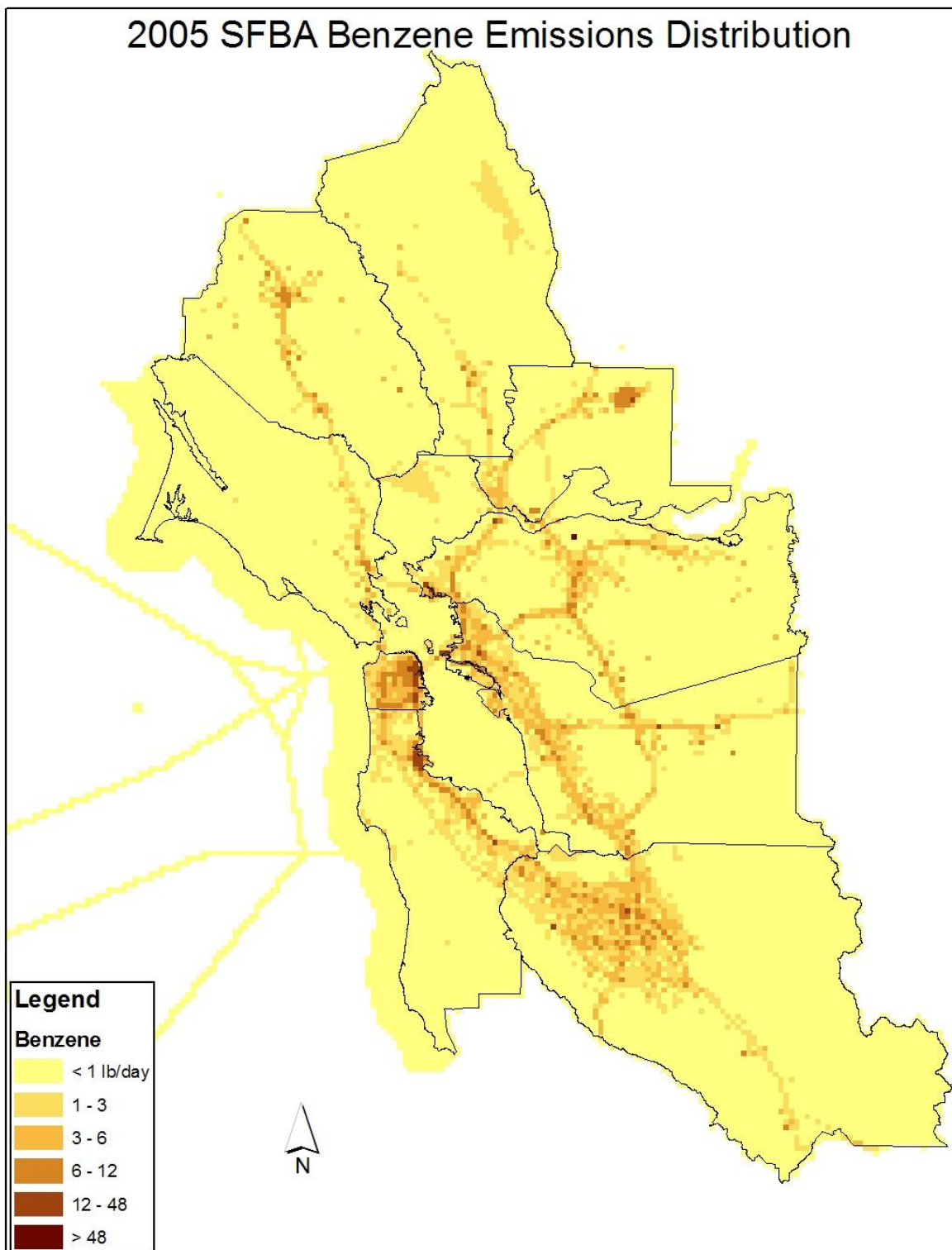


Figure A7: Spatial distribution of benzene emissions in the Bay Area.

APPENDIX B

Meteorological Model Verification

To evaluate the performance of MM5 simulation, we used ENVIRON's METSTAT program (Emery et al., 2001) to compare the MM5 predicted meteorological fields to the surface observations collected by the District meteorological observation network.

The METSTAT program is a statistical analysis software package that calculates and graphically presents the statistics, such as, mean observation, mean prediction, bias error, gross error, index of agreement (IOA), etc.

In this appendix, the hourly time series of observed and predicted surface-layer wind and temperature are presented to evaluate the model performance. The statistics measurements such as Mean Observation, Mean Prediction and Bias Error are defined as follows:

Mean Observation (M_o): calculated from all sites with valid data within a given analysis region and for a given time period (hourly or daily):

$$M_o = \frac{1}{IJ} \sum_{j=1}^J \sum_{i=1}^I O_j^i$$

where O_j^i is the individual observed quantity at site i and time j , and the summations are over all sites (I) and over time periods (J).

Mean Prediction (M_p): calculated from simulation results that are interpolated to each observation used to calculate the mean observation (hourly or daily):

$$M_p = \frac{1}{IJ} \sum_{j=1}^J \sum_{i=1}^I P_j^i$$

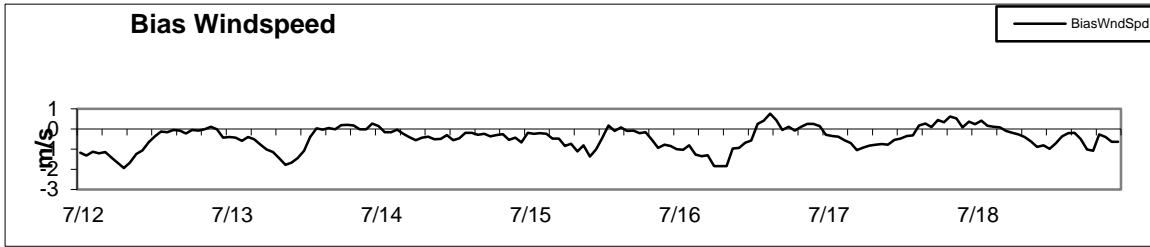
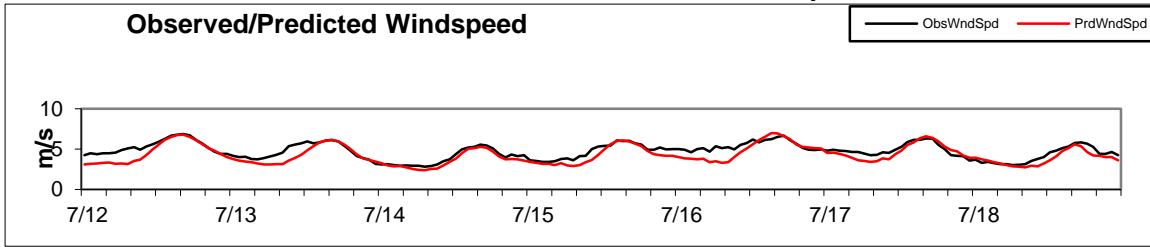
where P_j^i is the individual predicted quantity at site i and time j . Note that mean observed and predicted winds are vector-averaged (for east-west component u and north-south component v), from which the mean wind speed and mean resultant direction are derived.

Bias Error (B): calculated as the mean difference in prediction-observation pairings with valid data within a given analysis region and for a given time period (hourly or daily):

$$B = \frac{1}{IJ} \sum_{j=1}^J \sum_{i=1}^I (P_j^i - O_j^i)$$

The hourly time series of region-average observed and predicted surface-layer wind and temperature for July and December episodes of 2000 are shown in Figures B1a-B1c and B2a-B2c, respectively. The observations are from the Bay Area Meteorological network. The MM5 model results are averaged over both 1 and 4-km MM5 domains. The MM5 simulations show reasonably good agreement with the observations for wind speed, wind direction and temperature over both 1 and 4-km MM5 domains.

BAAQMD 1km 2000 MM5 -- July



BAAQMD 4km 2000 MM5 - July

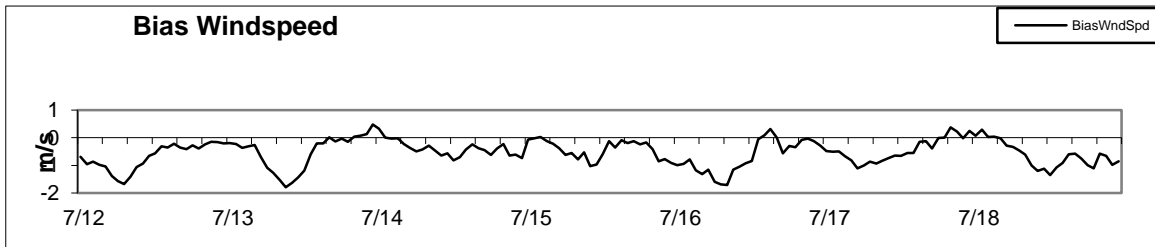
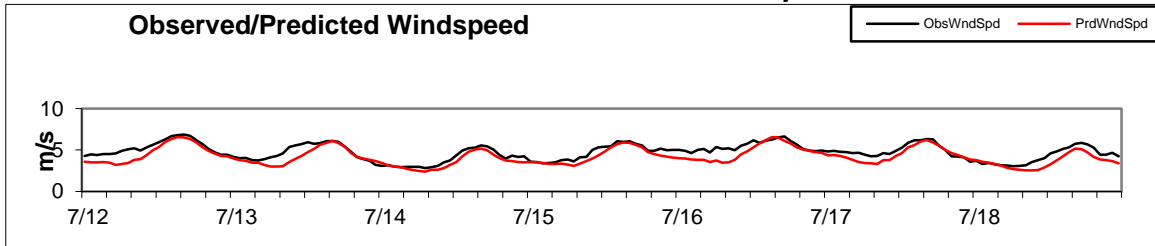
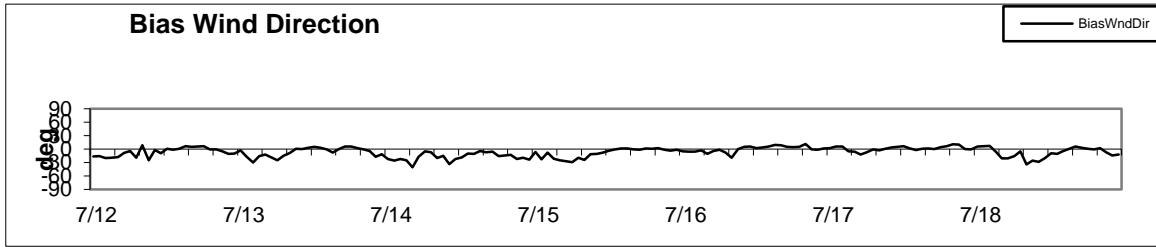
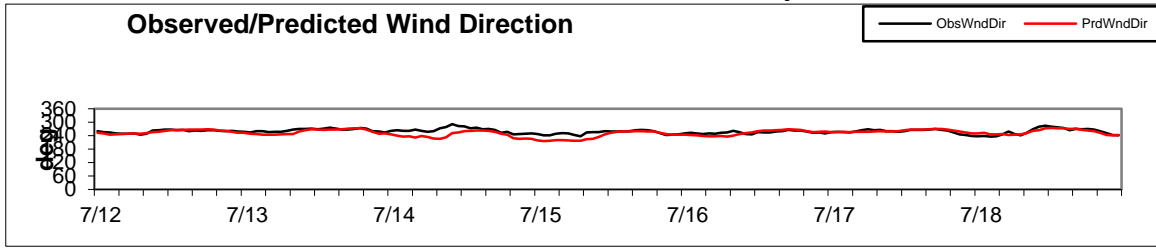


Figure B1a: Hourly time series of region-average observed and predicted surface-layer wind speed and performance statistics in the 1 and 4-km MM5 domains for July 12-18, 2000.

BAAQMD 1km 2000 MM5 -- July



BAAQMD 4km 2000 MM5 -- July

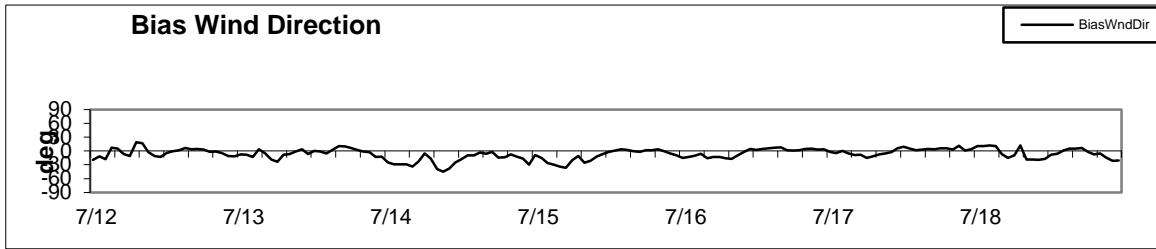
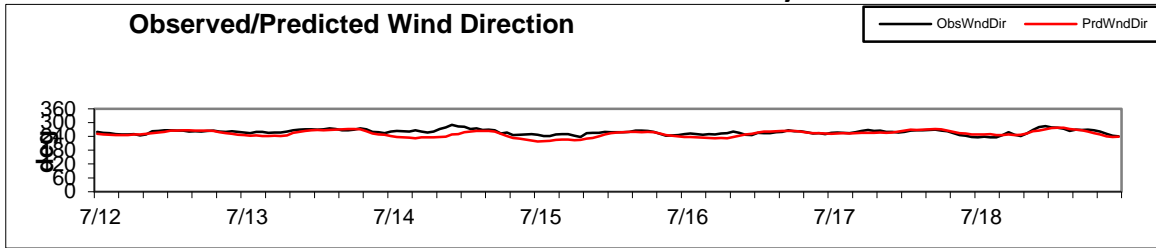
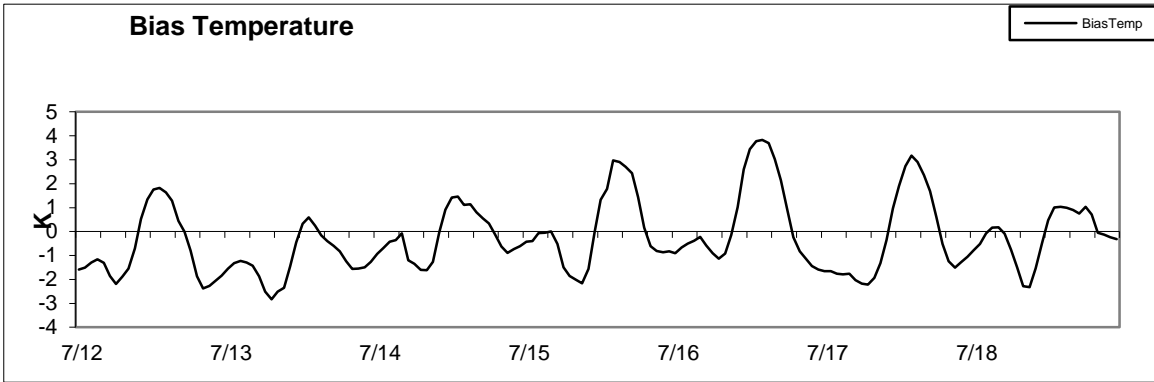
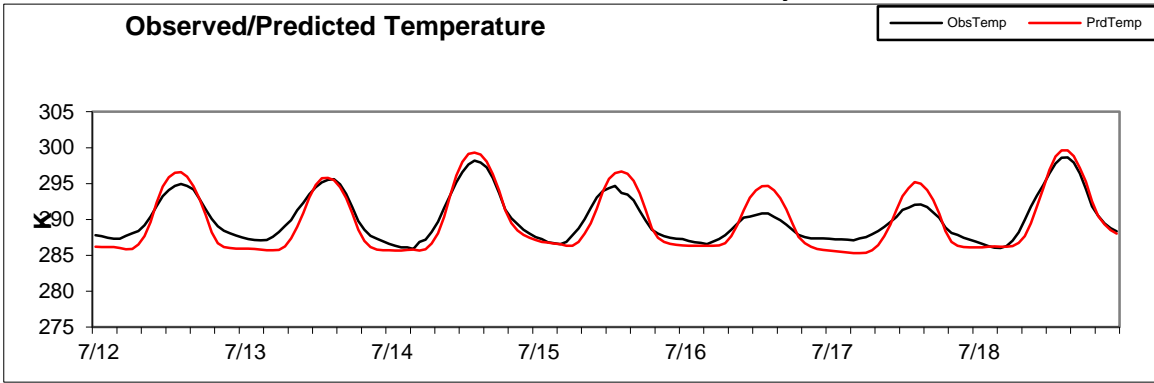


Figure B1b: Hourly time series of region-average observed and predicted surface-layer wind direction and performance statistics in the 1 and 4-km MM5 domains for July 12-18, 2000.

BAAQMD 1km 2000 MM5 -- July



BAAQMD 4km 2000 MM5 -- July

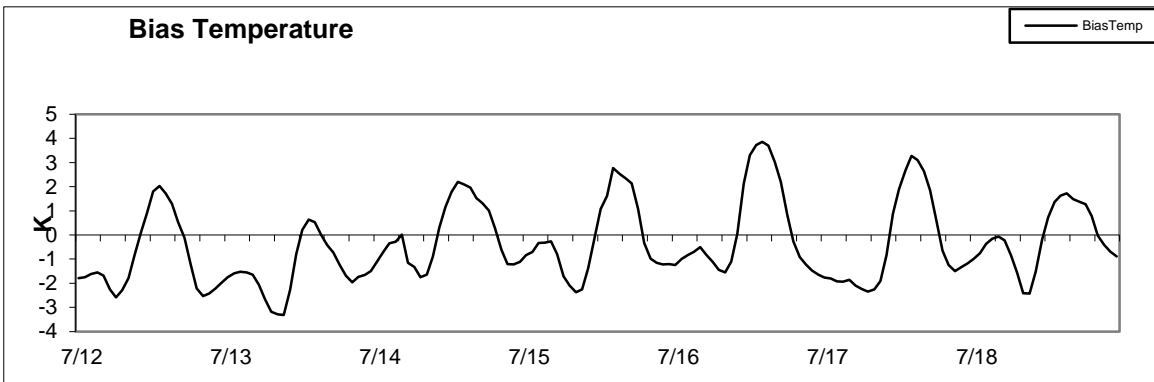
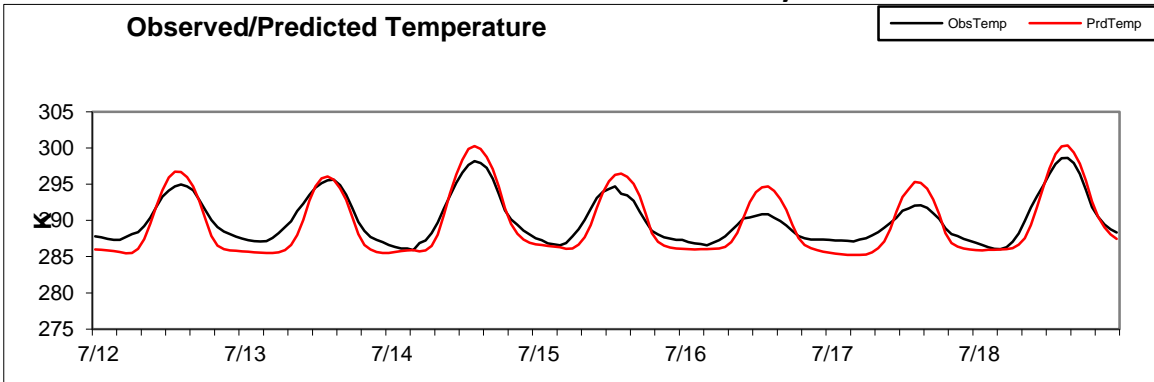


Figure B1c: Hourly time series of region-average observed and predicted surface-layer temperature and performance statistics in the 1 and 4-km MM5 domains for July 12-18, 2000.

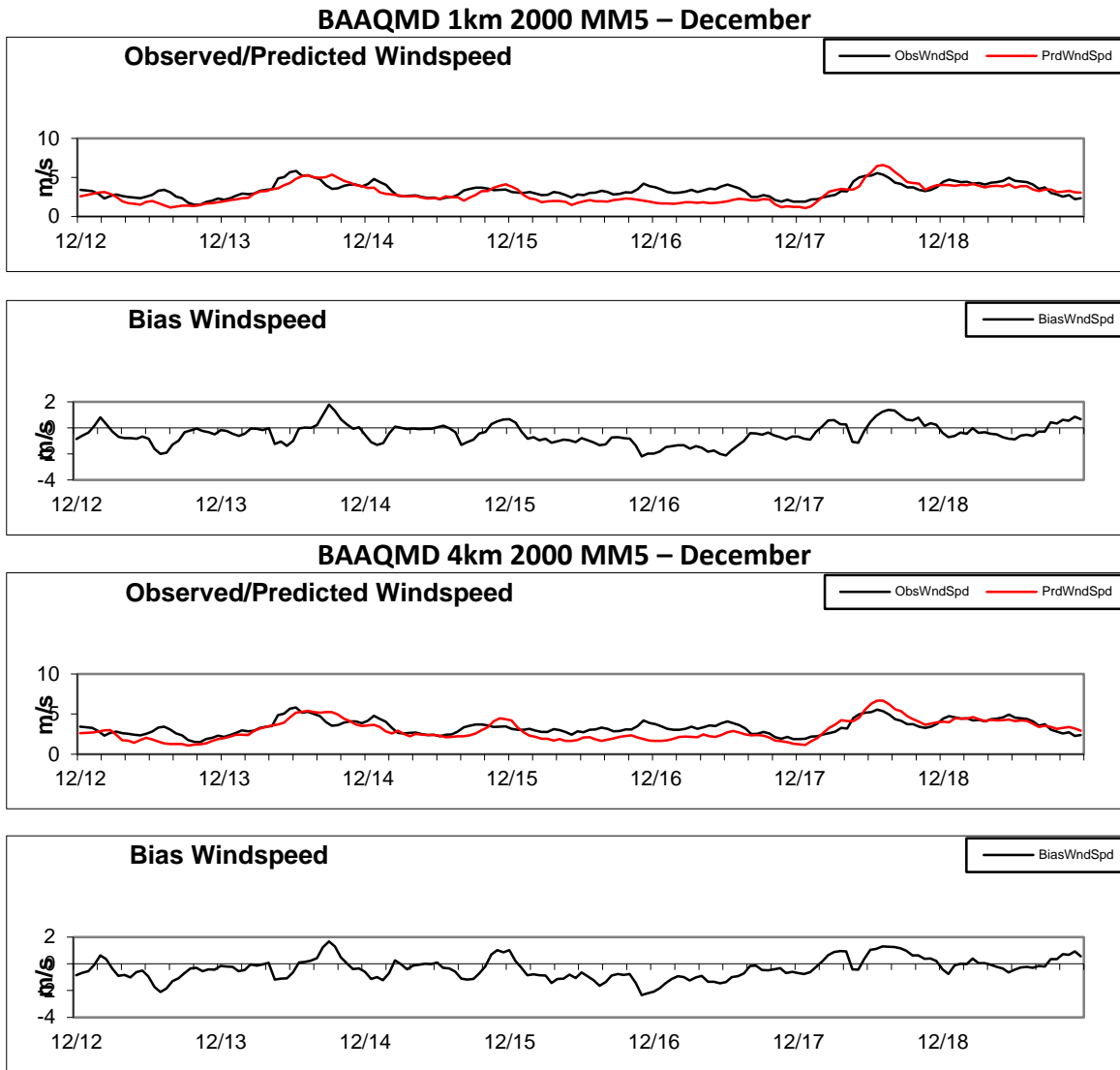


Figure B2a: Hourly time series of region-average observed and predicted surface-layer wind speed and performance statistics in the 1 and 4-km MM5 domains for December 12-18, 2000.

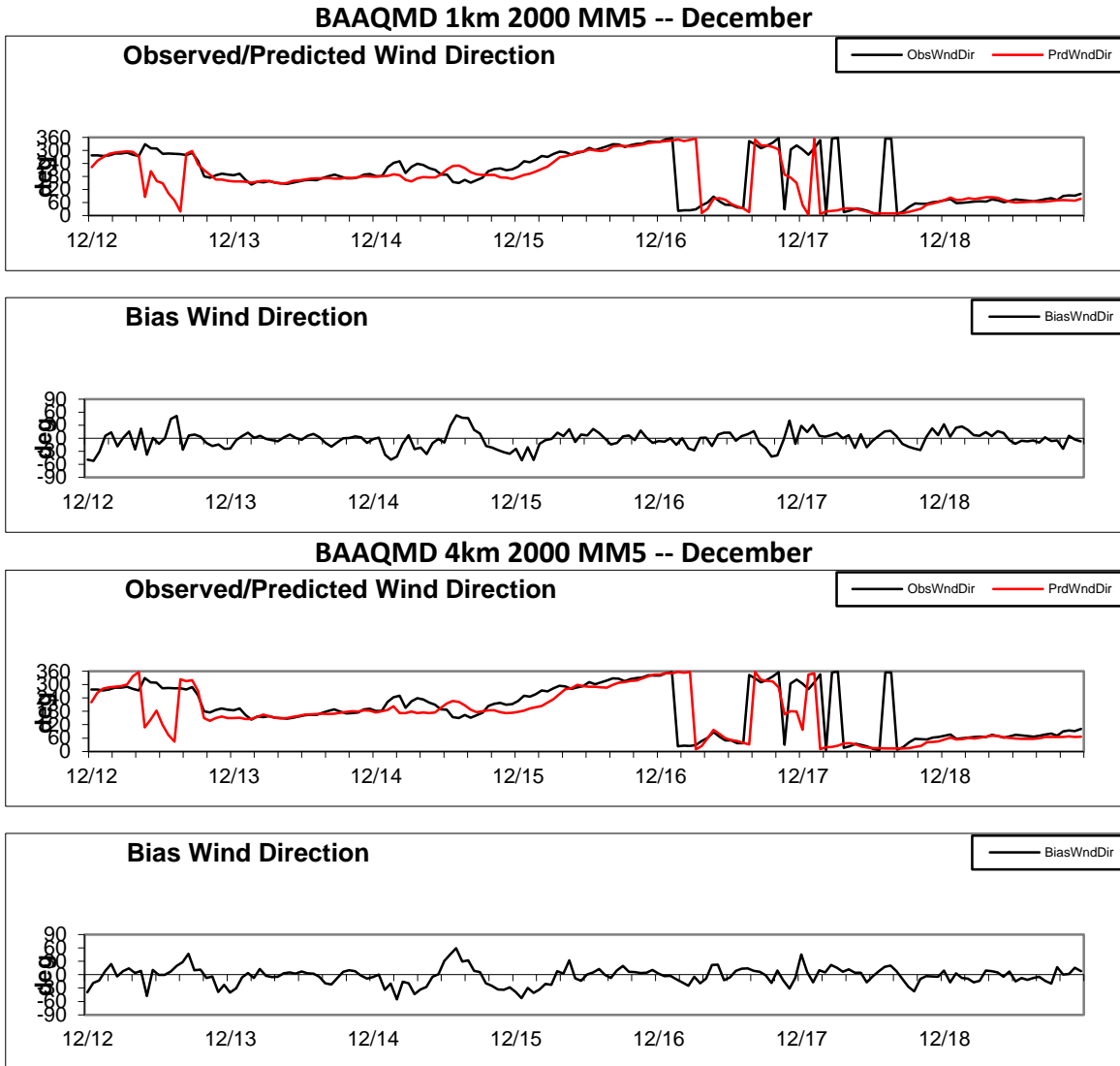
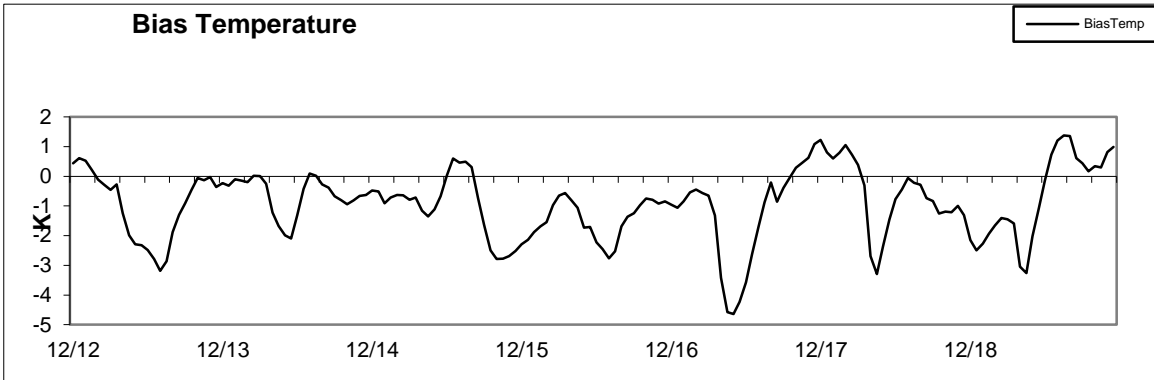
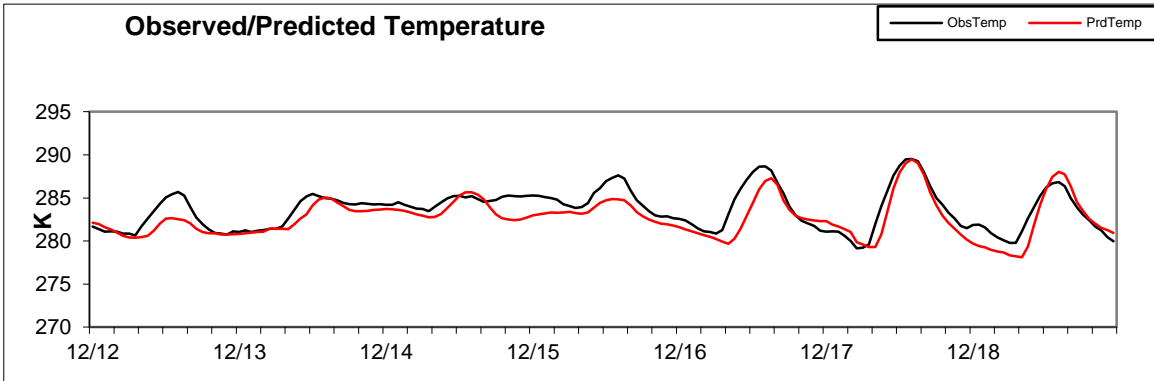


Figure B2b: Hourly time series of region-average observed and predicted surface-layer wind direction and performance statistics in the 1 and 4-km MM5 domains for December 12-18, 2000.

BAAQMD 1km 2000 MM5 – December



BAAQMD 4km 2000 MM5 -- December

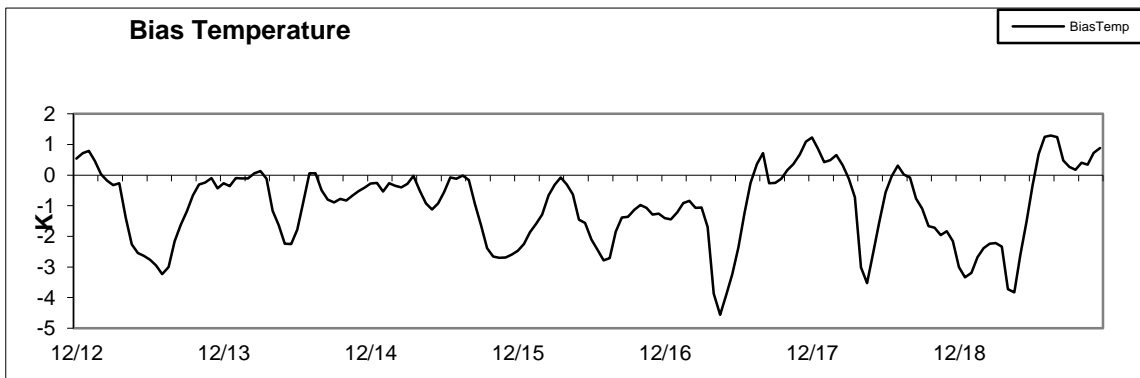
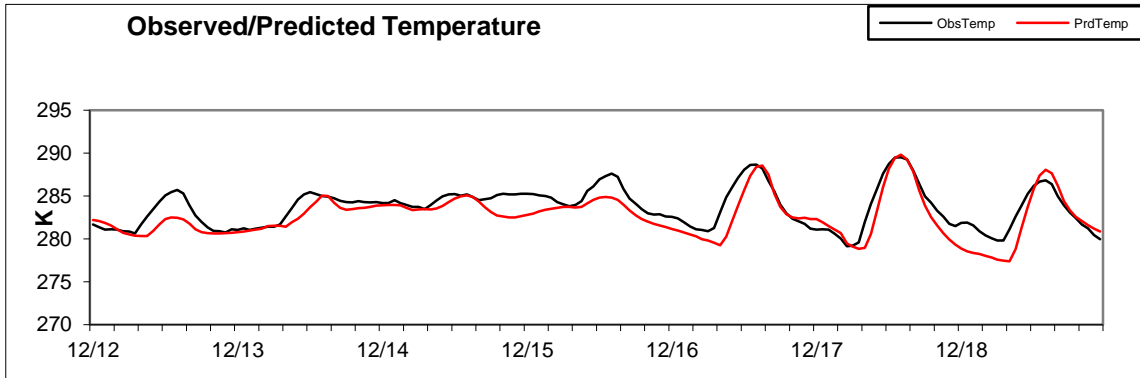


Figure B2c: Hourly time series of region-average observed and predicted surface-layer temperature and performance statistics in the 1 and 4-km MM5 domains for December 12-18, 2000.

APPENDIX C

Air Quality Model Evaluation

Air quality model performance was evaluated against available measurements of toxic air contaminants (TAC). Several assumptions were made. First, available TAC measurements were only collected on a one-day-in twelve schedule as 24-hour averages. To make meaningful comparisons, we derived seasonal (July and December) averages from the measurements over years 2004 through 2006 to compare with simulated seasonal averages near the measurement site. Since the simulation used emissions from year 2005 and meteorological inputs from 2000, the comparisons of seasonal averages can at best demonstrate similarity in magnitude, not matched agreement. In addition to comparing mean values, we examined the scatter from 24-hour measurements and compared to the scatter from daily averages of the simulated values near the measurement sites.

A second challenge to the model evaluation was that there were no direct measurements of diesel PM. As a surrogate, we used elemental carbon (EC) evaluated using the IMPROVE method. Specifically, using the modeled diesel concentration, we compared the July and December ambient concentrations of EC at the nine District sites having EC measurements with modeled fine diesel PM concentrations in the grid squares containing the site for those months.

To a first approximation, the results are consistent. The average across the nine sites is similar. For July, the modeled and ambient means are: 0.70 $\mu\text{g}/\text{m}^3$ and 0.55 $\mu\text{g}/\text{m}^3$. For December they are: 1.86 $\mu\text{g}/\text{m}^3$ and 2.10 $\mu\text{g}/\text{m}^3$.

Figure C1 shows a site by site comparison of seasonal means of modeled fine diesel PM versus observed ambient EC concentrations. In the legend of Figure C1, "Mod" represents modeled diesel PM concentrations, while "Amb" represents ambient observed EC values.

The comparison shows that modeled and observed July concentrations are close at a number of sites whose December observed levels are substantially higher: Vallejo, Concord, Napa, Bethel Island and Livermore. For Napa and maybe Vallejo, this might indicate that wood smoke is influencing the EC measurement. For the other sites, transport from the East, and possibly some EC wood smoke, might account for the differences. The modeling did not include diesel PM emissions outside the District, and boundary values were set to reflect annual average values.

Observed EC and simulated diesel PM at Point Reyes agree well in both July and December.

The San Francisco site is a large outlier, with modeled diesel PM three to four times observed EC concentrations. This could be an indication of a problem with the off-road vehicle inventory.

In general, we'd expect EC = diesel PM. EC is part of diesel exhaust, roughly 70-80%. For summer, the ratio of mean EC to mean modeled diesel is 0.78, conforming to expectations. But for winter the ratio is 1.13, suggesting other sources of EC, like wood smoke and transport.

Model Diesel vs. Ambient EC for December & July 2005-06

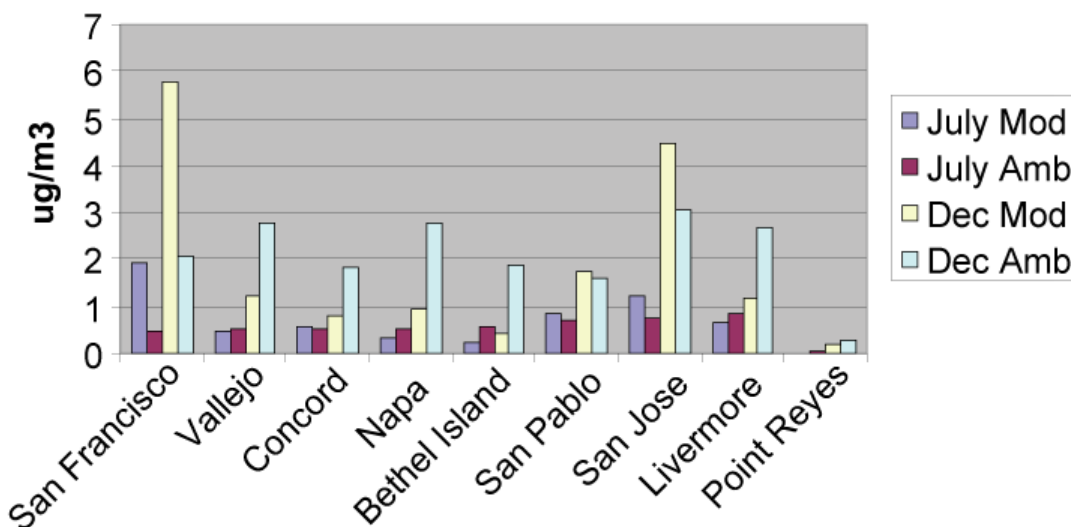


Figure C1: Modeled diesel particulate matter concentrations vs. observed ambient elemental carbon in July and December.

To evaluate the simulated reactive TAC, the mean and median simulated values of five toxics species (benzene, 1,3-butadiene, formaldehyde, acetaldehyde, and acrolein) were compared against observations. Observational data used for this comparison were taken from 2004 to 2006 for July and December. Because measurements are made only once every 12 days, there were only seven or eight measurements of a particular toxic species at a particular site for a specific month. Two tests (a student's t-test (for the mean) and a Wilcoxon test (for the median)) were applied.

As can be seen in Figures C2 and C3, the simulated values for benzene, 1,3-butadiene, formaldehyde, and acetaldehyde were generally not statistically different from the ambient. The modeled values for acrolein were generally smaller than ambient. There were significant differences in the model-ambient relationship between summer and winter.

For benzene and 1,3-butadiene, there was only one statistically significant difference between modeled and ambient values, a borderline difference for 1,3-butadiene for summer in San Jose. For formaldehyde, there was no statistically significant difference in

wintertime values, but the summertime modeled values were significantly lower than ambient. For acetaldehyde, the pattern was similar to formaldehyde, but only the summertime difference at Fremont was statistically significant, and San Francisco's wintertime modeled values were significantly higher than ambient. For acrolein, the July ambient values were far higher than modeled; the December ambient values were also higher than modeled, though closer.

Note: In the figures, two asterisks above a modeled-ambient pair indicates a highly significant difference (p -value < 0.01). One asterisk indicates a borderline significant difference (p -value ≥ 0.01 and < 0.05). The small sample sizes mean that there could be some relatively large differences between the model and ambient means and medians but that the test would not have the power to detect them; the tests where the modeled differed from the ambient by a factor of two or more were all statistically significant.

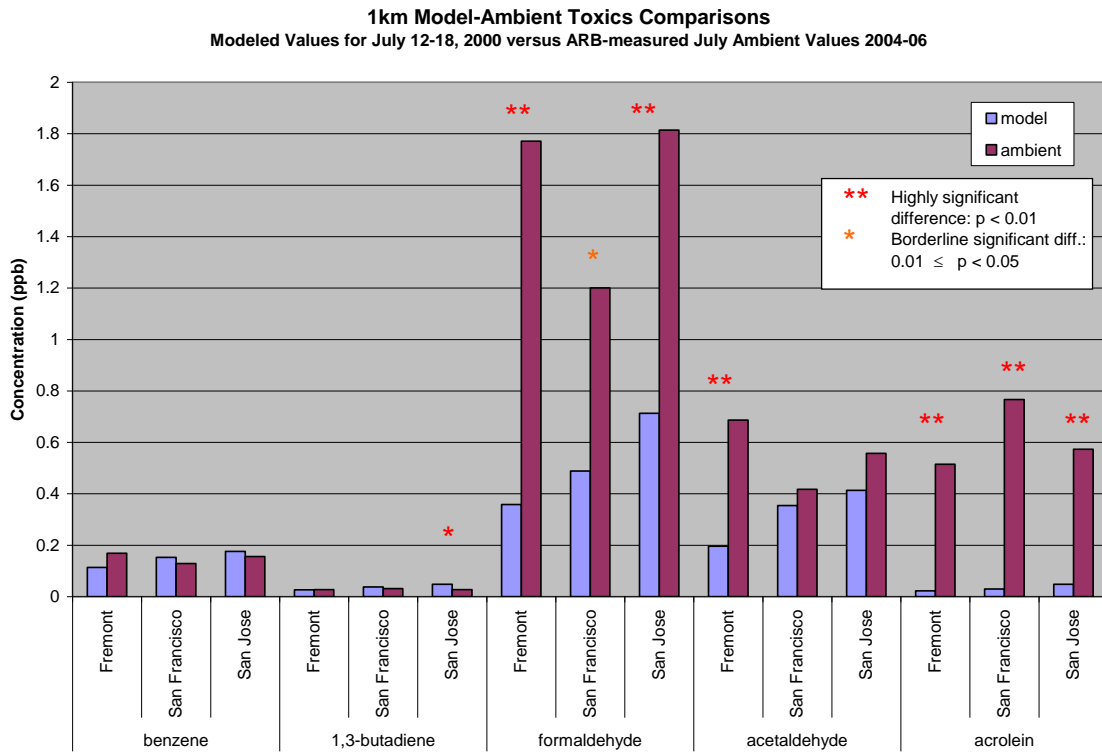


Figure C2: Modeled vs. ambient toxics comparison for July.

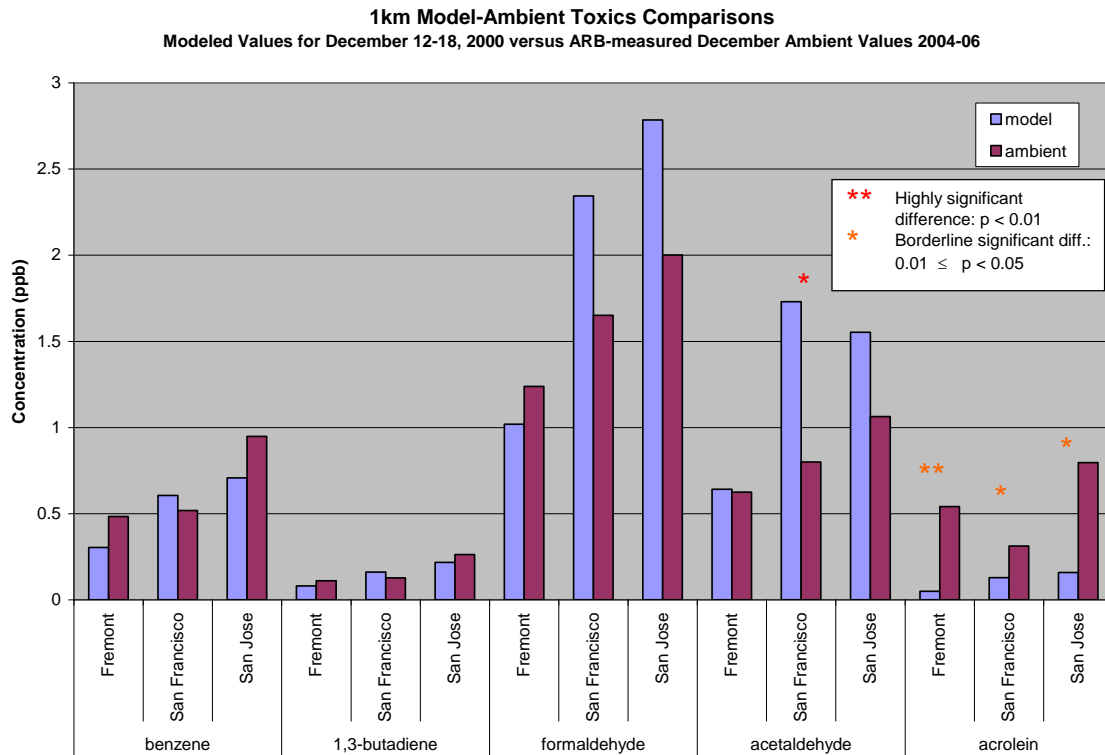


Figure C3: Modeled vs. ambient toxics comparison for December.

Day-to-day variability in the modeled species versus the variability in the ambient measurements was also investigated. Figures C4-C8 show that the modeled variability is generally less than that of the ambient. The modeled data are derived from two weeks in 2000, selected because they were typical, July 12-18, 2000 and December 12-18, 2000. The ambient data are from other days from all different weeks in those months and from weather conditions that are more or less random.

The graphs are presented in July-December pairs for each of the five toxics: benzene, 1,3-butadiene, formaldehyde, acetaldehyde and acrolein. Each graph presents comparisons of the modeled and ambient concentrations for 3 sites: Fremont, San Francisco, and San Jose.

The most obvious observation is that in every case, the July observations are less variable than the December observations, a characteristic that the model shares. The modeled values are less variable, with differences being statistically significant for most pollutants/seasons. The July modeled values are substantially smaller in every case, whereas the winter acetaldehyde values are not statistically different and the formaldehyde values only marginally different.

Note that, if the model is functioning appropriately, then its values should vary less than the individual measurements. This is because the model represents an average which,

mathematically, always has a smaller variance than the corresponding individual measured values.

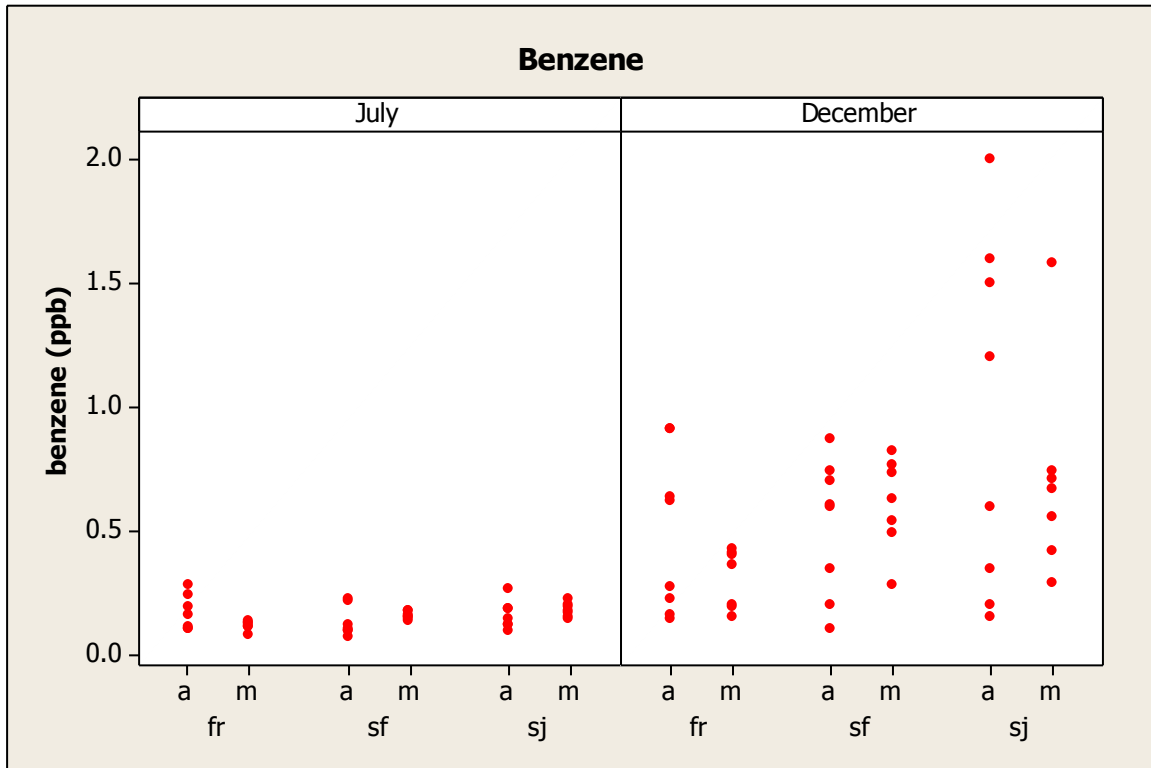


Figure C4: Comparison of modeled and ambient benzene for July and December. Labels a = ambient, m = modeled, fr = Fremont, sf = San Francisco, sj = San Jose.

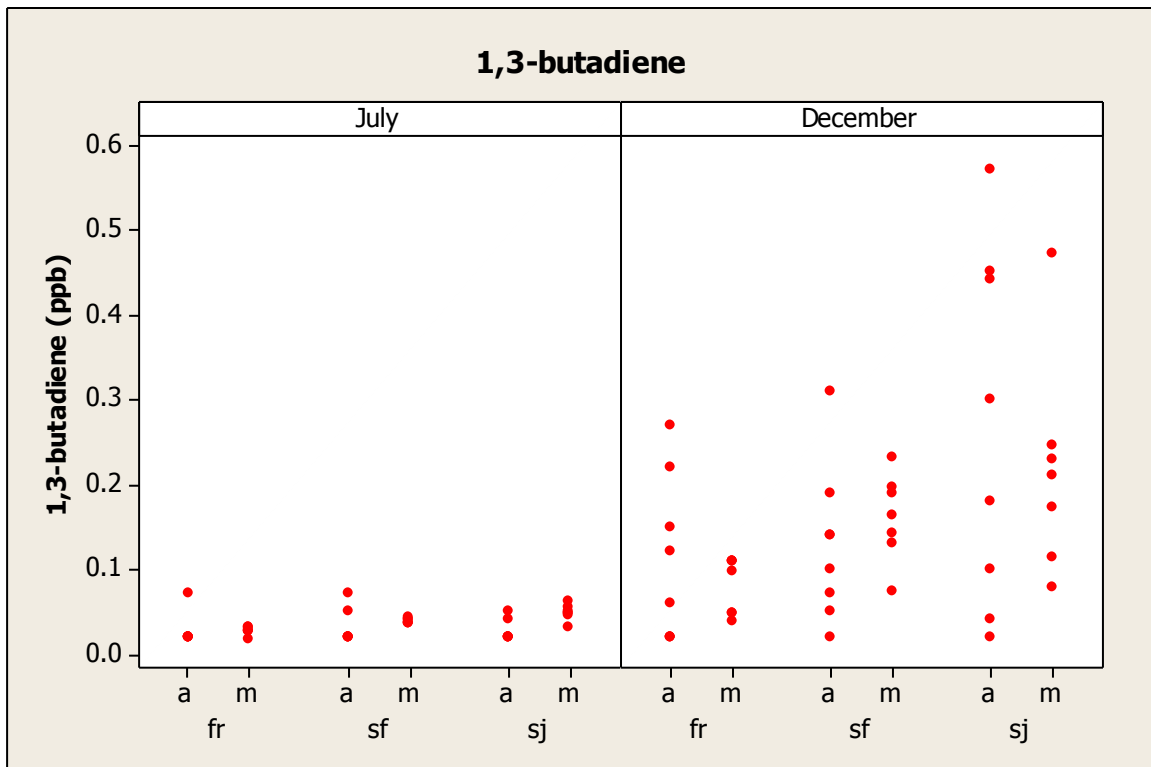


Figure C5: Comparison of modeled and ambient 1,3-butadiene for July and December. Labels a = ambient, m = modeled, fr = Fremont, sf = San Francisco, sj = San Jose.

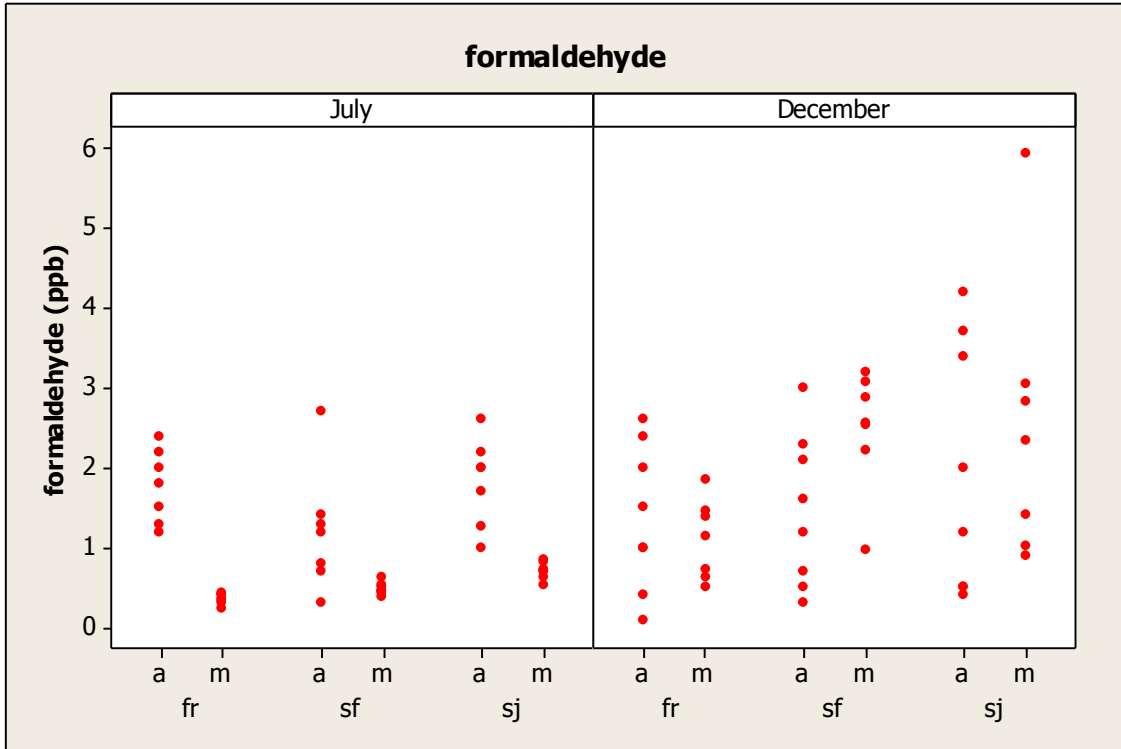


Figure C6: Comparison of modeled and ambient formaldehyde for July and December. Labels a = ambient, m = modeled, fr = Fremont, sf = San Francisco, sj = San Jose.

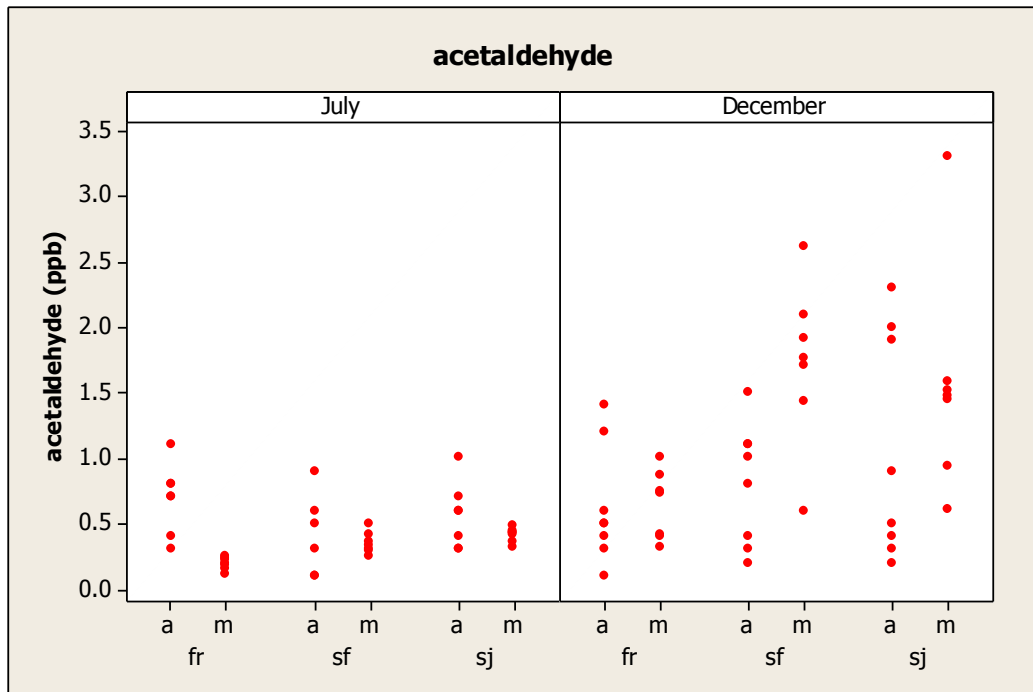


Figure C7: Comparison of modeled and ambient acetaldehyde for July and December. Labels: a = ambient, m = modeled, fr = Fremont, sf = San Francisco, and sj = San Jose.

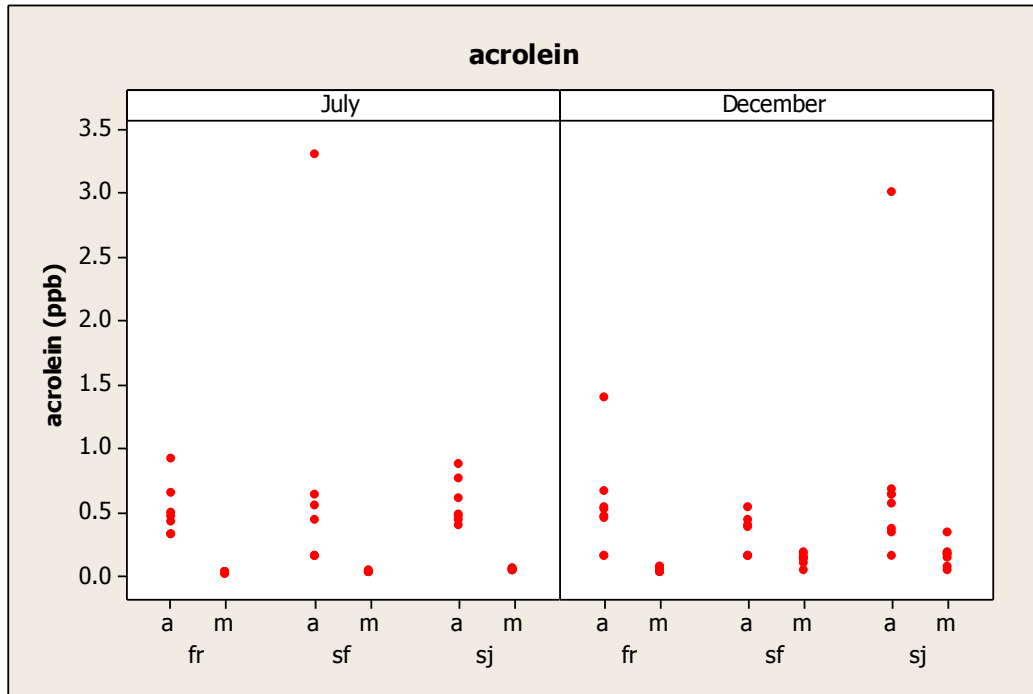


Figure C8: Comparison of modeled and ambient acrolein for July and December. Labels: a = ambient, m = modeled, fr = Fremont, sf = San Francisco, and sj = San Jose

APPENDIX D

Chemistry for Secondary Toxics Formation

The CAMx model, version 4.50, was used to predict concentrations of toxic air contaminants in the San Francisco Bay Area (Bay Area). The model was run in an inert tracer mode to predict diesel particulate matter (diesel PM) dispersion. In the inert mode, the model represented the dynamic processes of advection from the mean winds; turbulent diffusion, which approximates transport from transient, small-scale variations from the mean winds; and dry deposition. Chemical transformation and removal of diesel PM via chemical reactions was assumed to be negligible compared to other processes.

To simulate chemically reactive toxic air contaminants, the same version of CAMx was run with the SAPRC99 chemical mechanism coupled with the Reactive Tracer Chemical Mechanism Compiler (RTCMC) and the Reactive Tracer (RTRAC) modules (ENVIRON, 2008).

RTCMC allows users to input, in a text format, a set of chemical reactions for selected species to be treated by the CAMx Reactive Tracer (RTRAC) Probing Tool. RTRAC is then used within CAMx to simulate reactive tracers. RTCMC is the front-end to RTRAC that reads (and solves) a user-defined chemical mechanism for reactive tracers. The core model's photochemical mechanisms remain intact and separate from the reactive tracer chemistry. The RTCMC module allows a user-defined toxic chemistry mechanism to run in parallel with, and to draw oxidant information from, a standard gas-phase photochemical simulation (i.e., using CB05 or SAPRC99 chemical mechanisms). A suitable application for RTCMC is simulating air toxic species that are photolyzed and/or decay according to ambient concentrations of ozone, OH, NO, etc.

The SAPRC99 chemistry was applied as it would be for a standard gas-phase photochemical simulation to supply highly reactive oxidant and radical compounds—such as ozone, hydroxyl and peroxy radicals—and some toxic compounds that are represented explicitly in the SAPRC99 mechanism, such as formaldehyde and acetaldehyde.

The user defines a complete toxics chemical mechanism in an ASCII format (examples are provided below). Upon startup, CAMx/RTCMC compiles the information and configures the reactive tracer chemistry solver to numerically solve the toxics mechanism. During the model simulation, the toxics chemistry receives ambient pollutant information from the core photochemical mechanism and uses this to calculate the concentrations of toxic species. The current implementation of RTCMC is for gas-phase reactions, i.e., gas-phase tracers reacting with each other and/or gas-phase host model species. The text input file format is described elsewhere (ENVIRON, 2008) and an example is provided in Listing D1 below.

```

#Control
  rate_species_units = 'molecules/cm3'
  rate_time_units = 'sec'
  solver = 'dlsode'
  Jacobian = 'numeric'
#Species,Type,Ambient,Tolerance,deposition vel,wet scav,mw,ldos,ldep
O3      A      0.0      1.0E-12  0.0  0.0  1.0
NO      A      0.0      1.0E-12  0.0  0.0  1.0
NO2     A      0.0      1.0E-12  0.0  0.0  1.0
OH      A      0.0      1.0E-12  0.0  0.0  1.0
HO2     A      0.0      1.0E-12  0.0  0.0  1.0
NO3     A      0.0      1.0E-12  0.0  0.0  1.0
CXO2    A      0.0      1.0E-12  0.0  0.0  1.0
BUTD    F      0.0      1.0E-12  0.0  0.0  1.0
BUO2_A  F      0.0      1.0E-12  0.0  0.0  1.0
BUO2_B  F      0.0      1.0E-12  0.0  0.0  1.0
SACR    F      0.0      1.0E-12  0.0  0.0  1.0
ACR     F      0.0      1.0E-12  0.0  0.0  1.0
PFRM    F      0.0      1.0E-12  0.0  0.0  1.0
SFRM    F      0.0      1.0E-12  0.0  0.0  1.0
C2H4    F      0.0      1.0E-12  0.0  0.0  1.0
NPRD    F      0.0      1.0E-12  0.0  0.0  1.0
DIOL    F      0.0      1.0E-12  0.0  0.0  1.0
BUPX_A  F      0.0      1.0E-12  0.0  0.0  1.0
HBAL    F      0.0      1.0E-12  0.0  0.0  1.0
HBO2    F      0.0      1.0E-12  0.0  0.0  1.0
HBPX    F      0.0      1.0E-12  0.0  0.0  1.0
BUPX_B  F      0.0      1.0E-12  0.0  0.0  1.0
GLAL    F      0.0      1.0E-12  0.0  0.0  1.0
GXAL    F      0.0      1.0E-12  0.0  0.0  1.0
ACO3    F      0.0      1.0E-12  0.0  0.0  1.0
ACPN    F      0.0      1.0E-12  0.0  0.0  1.0
ACCA    F      0.0      1.0E-12  0.0  0.0  1.0
ACPA    F      0.0      1.0E-12  0.0  0.0  1.0
HBO3    F      0.0      1.0E-12  0.0  0.0  1.0
HBPN    F      0.0      1.0E-12  0.0  0.0  1.0
HBCA    F      0.0      1.0E-12  0.0  0.0  1.0
HBPA    F      0.0      1.0E-12  0.0  0.0  1.0
ATAL    F      0.0      1.0E-12  0.0  0.0  1.0
ATO3    F      0.0      1.0E-12  0.0  0.0  1.0
ATPN    F      0.0      1.0E-12  0.0  0.0  1.0
ATCA    F      0.0      1.0E-12  0.0  0.0  1.0
ATPA    F      0.0      1.0E-12  0.0  0.0  1.0
C1O2    F      0.0      1.0E-12  0.0  0.0  1.0
C1PX    F      0.0      1.0E-12  0.0  0.0  1.0
BENZ    F      0.0      1.0E-12  0.0  0.0  1.0
#Table
  0      0.      10.     20.     30.     40.     50.     60.     70.     78.     86.
12 4.125E-04 4.071E-04 3.899E-04 3.615E-04 3.195E-04 2.629E-04 1.920E-04 1.101E-04 4.903E-05 1.112E-05
15 4.125E-04 4.071E-04 3.899E-04 3.615E-04 3.195E-04 2.629E-04 1.920E-04 1.101E-04 4.903E-05 1.112E-05
19 3.313E-02 3.284E-02 3.189E-02 3.025E-02 2.768E-02 2.392E-02 1.870E-02 1.176E-02 5.688E-03 1.384E-03
30 1.527E-03 1.497E-03 1.404E-03 1.254E-03 1.046E-03 7.885E-04 5.053E-04 2.373E-04 8.485E-05 1.484E-05
43 1.527E-03 1.497E-03 1.404E-03 1.254E-03 1.046E-03 7.885E-04 5.053E-04 2.373E-04 8.485E-05 1.484E-05
46 1.527E-03 1.497E-03 1.404E-03 1.254E-03 1.046E-03 7.885E-04 5.053E-04 2.373E-04 8.485E-05 1.484E-05
49 8.344E-03 8.267E-03 8.019E-03 7.597E-03 6.953E-03 6.035E-03 4.787E-03 3.124E-03 1.583E-03 3.598E-04
55 3.333E-03 3.297E-03 3.185E-03 2.993E-03 2.697E-03 2.278E-03 1.718E-03 1.021E-03 4.670E-04 1.095E-04
56 2.502E-03 2.463E-03 2.341E-03 2.141E-03 1.850E-03 1.468E-03 1.011E-03 5.247E-04 2.074E-04 4.005E-05
62 4.555E-04 4.452E-04 4.138E-04 3.642E-04 2.962E-04 2.147E-04 1.292E-04 5.463E-05 1.709E-05 2.522E-06
73 4.125E-04 4.071E-04 3.899E-04 3.615E-04 3.195E-04 2.629E-04 1.920E-04 1.101E-04 4.903E-05 1.112E-05
76 3.333E-03 3.297E-03 3.185E-03 2.993E-03 2.697E-03 2.278E-03 1.718E-03 1.021E-03 4.670E-04 1.095E-04
77 2.502E-03 2.463E-03 2.341E-03 2.141E-03 1.850E-03 1.468E-03 1.011E-03 5.247E-04 2.074E-04 4.005E-05
81 3.313E-02 3.284E-02 3.189E-02 3.025E-02 2.768E-02 2.392E-02 1.870E-02 1.176E-02 5.688E-03 1.384E-03
#Equations
  1 [BUTD] + [OH] ->(0.78)[BUO2_A] + (0.22)[BUO2_B] ; 2 1.48E-11 448. 0.
  2 [BUTD] + [O3] ->(0.62)[SACR] + (0.83)[SFRM] + (0.17)[C2H4] ; 2 1.34E-14 -2283. 0.
  3 [BUTD] + [NO3] -> [NPRD] ; 1 1.03E-13
  4 [BUO2_A] + [NO] ->(0.95)[SACR] + (0.95)[SFRM] + (0.05)[NPRD] ; 2 2.54E-12 360. 0.
  5 [BUO2_A] + [CXO2] ->(0.8)[SACR] + (0.8)[SFRM] + (0.2)[DIOL] ; 1 2.0E-12
  6 [BUO2_A] + [HO2] -> [BUPX_A] ; 2 1.8E-13 1300. 0.
  7 [BUO2_B] + [NO] ->(0.95)[HBAL] + (0.05)[NPRD] ; 2 2.54E-12 360. 0.
  8 [BUO2_B] + [CXO2] ->(0.8)[HBAL] + (0.2)[DIOL] ; 1 2.0E-12
  9 [BUO2_B] + [HO2] -> [BUPX_B] ; 2 1.8E-13 1300. 0.
 10 [BUPX_A] + [OH] -> [SACR] + [SFRM] ; 1 8.0E-11
 11 [BUPX_A] + [O3] -> [GLAL] + [SFRM] ; 1 8.0E-18
 12 [BUPX_A] -> [SACR] ; 0 0.0
 13 [BUPX_B] + [OH] -> [GLAL] + [GXAL] ; 1 8.0E-11

```

```

14 [BUPX_B] + [O3] -> [GLAL] + [SFRM] ;1 8.0E-18
15 [BUPX_B] -> [HBAL] ;0 0.0
16 [SACR] + [OH] -> [ACO3] ;1 1.5E-11
17 [SACR] + [O3] ->(0.6)[GXAL] +(0.8)[SFRM] ;1 2.9E-19
18 [SACR] + [NO3] -> [ACO3] ;2 1.73E-12 -1862. 0.
19 [SACR] ->(0.5)[ACO3] +(0.5)[SFRM] ;0 0.0
20 [ACO3] + [NO] ->(0.95)[SFRM] +(0.05)[NPRD] ;2 2.54E-12 360. 0.
21 [ACO3] + [CXO2] ->(0.7)[SFRM] +(0.3)[ACCA] ;1 1.00E-11
22 [ACO3] + [HO2] ->(0.7)[ACPA] +(0.3)[ACCA] ;2 2.91E-13 1300. 0.
23 [ACO3] + [NO2] -> [ACPNI] ;3 1.00E-05 8.9 2.41E-11 0.2
24 [ACPNI] -> [ACO3] + [NO2] ;8 23 1.11E+28 -14000.
25 [ACCA] + [OH] -> [SFRM] ;1 8.66E-12
26 [ACPA] + [OH] -> [ACO3] ;1 1.22E-11
27 [HBAL] + [OH] ->(0.57)[HBO3] +(0.43)[HBO2] ;1 3.87E-11
28 [HBAL] + [O3] ->(0.6)[GLAL] +(0.6)[GXAL] +(0.1)[SFRM] ;1 9.60E-18
29 [HBAL] + [NO3] -> [HBO3] ;2 1.44E-12 -1862. 0.
30 [HBAL] -> [GLAL] ;0 0.0
31 [HBO3] + [NO] ->(0.95)[GLAL] +(0.05)[NPRD] ;2 2.54E-12 360. 0.
32 [HBO3] + [CXO2] ->(0.7)[GLAL] +(0.3)[HBCA] ;1 1.00E-11
33 [HBO3] + [HO2] ->(0.7)[HBPX] +(0.3)[HBCA] ;2 2.91E-13 1300. 0.
34 [HBO3] + [NO2] -> [HBPN] ;3 1.00E-05 8.9 2.41E-11 0.2
35 [HBPN] -> [HBO3] + [NO2] ;8 34 1.11E+28 -14000.
36 [HBCA] + [OH] -> [GLAL] ;1 8.66E-12
37 [HBPX] + [OH] -> [HBO3] ;1 1.22E-11
38 [HBO2] + [NO] ->(0.98)[GXAL] +(0.98)[GLAL] +(0.02)[NPRD] ;2 2.54E-12 360. 0.
39 [HBO2] + [CXO2] ->(0.6)[GXAL] +(0.6)[GLAL] +(0.4)[DIOL] ;1 2.00E-12
40 [HBO2] + [HO2] -> [HBPX] ;2 2.91E-13 1300. 0.
41 [HBPX] + [OH] -> [GLAL] ;1 8.0E-11
42 [HBPX] + [NO3] -> [GLAL] ;2 1.44E-12 -1862. 0.
43 [HBPX] -> [GLAL] ;0 0.0
44 [GLAL] + [OH] ->(0.8)[SFRM] +(0.2)[GXAL] ;1 8.0E-12
45 [GLAL] + [NO3] -> [SFRM] ;2 1.44E-12 -1862. 0.
46 [GLAL] -> [SFRM] ;0 0.0
47 [GXAL] + [OH] -> ;1 1.1E-11
48 [GXAL] + [NO3] -> ;2 1.44E-12 -1862. 0.
49 [GXAL] -> ;0 0.0
50 [C2H4] + [OH] -> ;1 8.1E-12
51 [C2H4] + [O3] ->(1.37)[SFRM] ;2 9.14E-15 -2580. 0.
52 [C2H4] + [NO3] -> [SFRM] ;1 2.10E-16
53 [SFRM] + [OH] -> ;2 5.4E-12 -135. 0.
54 [SFRM] + [NO3] -> ;1 5.80E-16
55 [SFRM] -> ;0 0.0
56 [SFRM] -> ;0 0.0
57 [NPRD] + [OH] -> [SFRM] ;1 1.0E-12
58 [DIOL] + [OH] -> [GLAL] ;1 8.0E-12
59 [BENZ] + [OH] -> ;2 3.8E-12 -300. 0.
60 [ATAL] + [OH] -> [ATO3] ;2 5.6E-12 270. 0.
61 [ATAL] + [NO3] -> [ATO3] ;2 1.4E-12 -1900. 0.
62 [ATAL] -> [ATO3] ;0 0.0
63 [ATO3] + [NO] -> [C1O2] ;2 8.1E-12 270. 0.
64 [ATO3] + [CXO2] -> [C1O2] ;2 2.0E-12 500. 0.
65 [ATO3] + [NO2] -> [ATPN] ;3 7.22E-15 5.6 4.83E-08 1.5
66 [ATPN] -> [ATO3] + [NO2] ;8 65 1.11E+28 -14000.
67 [ATO3] + [HO2] ->(0.4)[ATPA] +(0.1)[ATCA] +(0.5)[C1O2] ;2 4.3E-13 1040. 0.
68 [ATPA] + [OH] -> [ATO3] ;2 4.0E-13 200. 0.
69 [C1O2] + [NO] -> [SFRM] ;2 2.8E-12 300. 0.
70 [C1O2] + [CXO2] -> [SFRM] ;2 9.5E-14 390. 0.
71 [C1O2] + [HO2] -> [C1PX] ;2 4.1E-13 750. 0.
72 [C1PX] + [OH] -> [SFRM] ;2 3.8E-12 200. 0.
73 [C1PX] -> [SFRM] ;0 0.0
74 [PFRM] + [OH] -> ;2 5.4E-12 -135. 0.
75 [PFRM] + [NO3] -> ;1 5.80E-16
76 [PFRM] -> ;0 0.0
77 [PFRM] -> ;0 0.0
78 [ACR] + [OH] -> [ACO3] ;1 1.5E-11
79 [ACR] + [O3] ->(0.6)[GXAL] +(0.8)[SFRM] ;1 2.9E-19
80 [ACR] + [NO3] -> [ACO3] ;2 1.73E-12 -1862. 0.
81 [ACR] ->(0.5)[ACO3] +(0.5)[SFRM] ;0 0.0

```

Listing D1. Example ASCII input file to the CAMx model using the Reactive Tracer Chemistry Mechanism Compiler.

APPENDIX E

Estimating Annual Diesel Concentrations

Since diesel surrogate, EC, appears to have another source, woodsmoke, during winter, we used CO as an alternative. CO appears to track modeled diesel better. The ratio of the annual CO mean to the July+December average is 0.96. Applying this ratio to the average July+December modeled diesel for the 8 District sites measuring OC/EC yields 1.37 $\mu\text{g}/\text{m}^3$.

Another approach is to consider a population-weighted average diesel. The county results seem reasonable except for San Francisco. If we arbitrarily cut SF's concentrations in half, then the population-weighted diesel concentrations are 2.0 $\mu\text{g}/\text{m}^3$ for December and 0.7 $\mu\text{g}/\text{m}^3$ for July. Taking the average and applying the 0.96 ratio yields an estimated population-weighted annual diesel concentration of 1.3 $\mu\text{g}/\text{m}^3$.

Some Details

Figure E1 compares modeled diesel December to July ratios with ambient CO and EC ratios. The modeled ratios are generally similar to the CO ratios, but the EC ratios are consistently higher. As discussed previously, this could be the effect of winter woodburning pushing the December EC means higher.

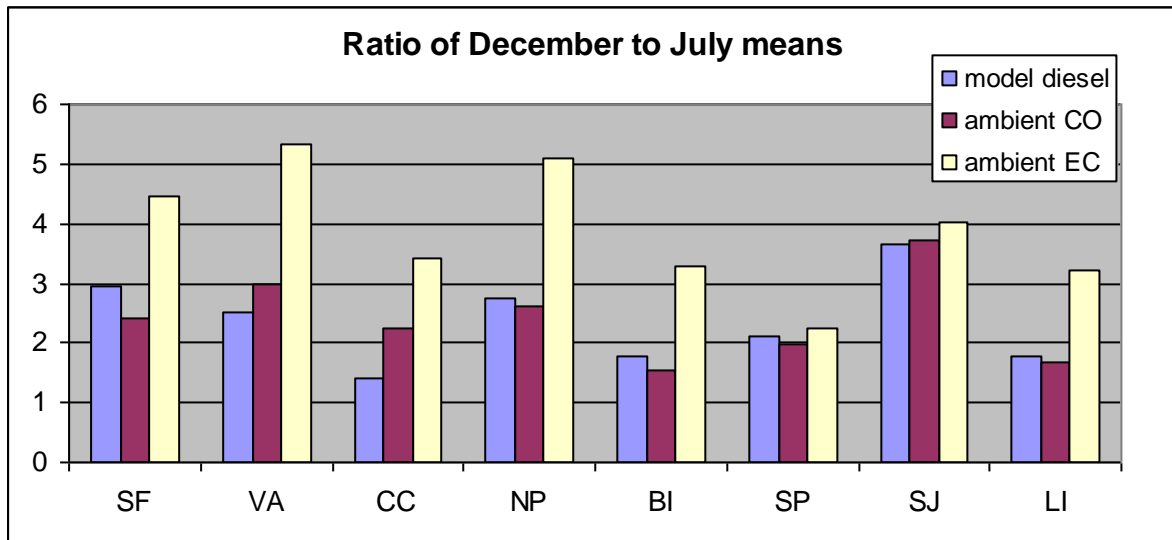


Figure E1: Ratio of December to July means.

This suggests that, to a first approximation, the seasonal pattern for CO is similar to the seasonal pattern for modeled diesel. So the relationship of annual CO to July+December CO provides a way to estimate annual diesel concentrations from the July and December averages. Figure E2 compares the annual CO means with the July+December averages at various District sites.

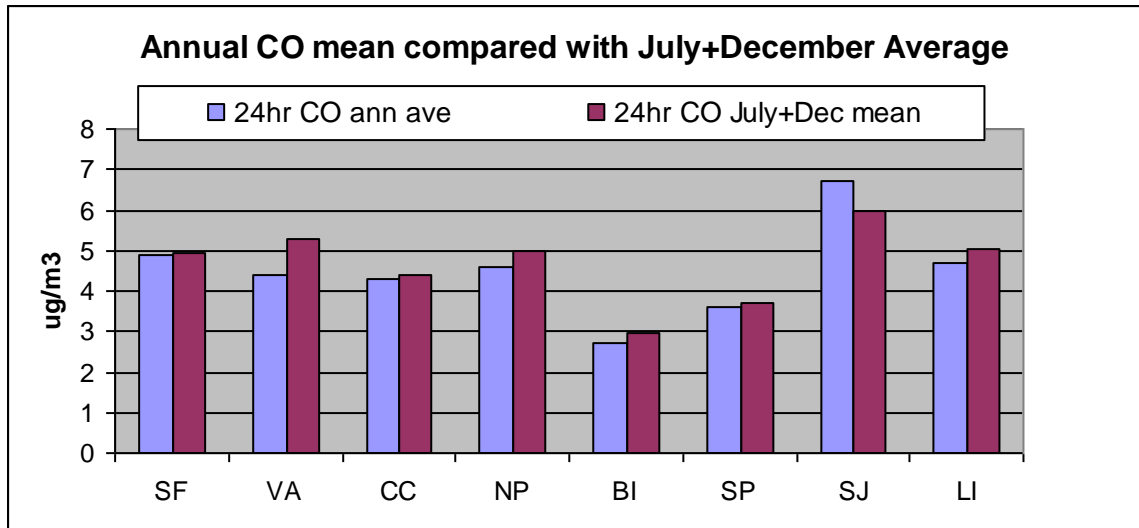


Figure E2: Annual CO mean compared with July+December averages.

The figure shows that the July+December CO mean is somewhat higher than the annual average at every site except San Jose. The ratio of the 8-site mean annual average to the 8-site mean July+December average is 0.96. Applying this factor to the mean of the modeled 8-site July+December diesel average yields an estimated Bay Area diesel annual mean concentration of 1.37 $\mu\text{g}/\text{m}^3$.

Taking the average of the 8 sites seemed somewhat arbitrary. To find a population-weighted diesel average, a program that cycles through Bay Area census tracts and multiplies the population of the tract times the estimated modeled diesel in the grid square containing the tract centroid was applied.

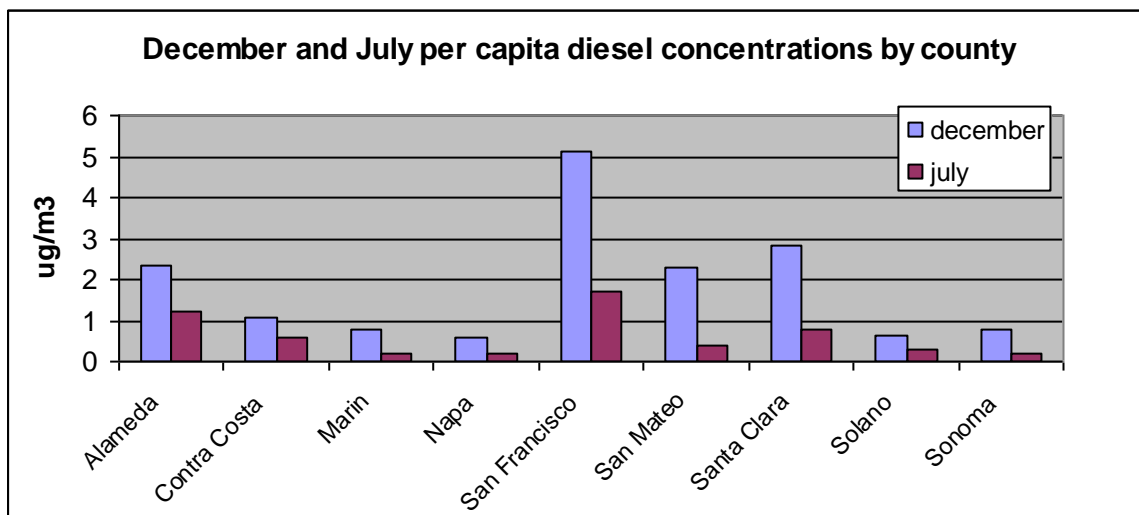


Figure E3: December and July per capita concentrations by county.

Figure E3 shows the resulting population-weighted concentrations by county. The values seem reasonable with the exception of San Francisco. As mentioned previously, the modeled results for SF far exceed the EC concentrations and are very possibly the result of

overestimation of off-road diesel. Therefore, SF concentrations were arbitrarily cut by 50%. Then, the estimated average Bay Area total population-weighted concentrations become 2.0 $\mu\text{g}/\text{m}^3$ for December and 0.7 $\mu\text{g}/\text{m}^3$ for July. Averaging these and applying the 0.96 factor yields an estimate that the Bay Area annual average population-weighted diesel exposure is 1.3 $\mu\text{g}/\text{m}^3$.